RSC Advances

PAPER

View Article Online
View Journal | View Issue

Cite this: *RSC Adv.*, 2024, **14**, 31126

Cutting-edge biomaterials for advanced biomedical uses: self-gelation of L-arginine-loaded chitosan/PVA/vanillin hydrogel for accelerating topical wound healing and skin regeneration†

Rabab M. Ibrahim,[a] Elbadawy A. Kamoun,[*bc] Noha M. Badawi,[d] Shahira H. EL-Moslamy,[e] Mahmoud kh.[f] and Samar A. Salim[*a]

The self-gelation utilizes natural vanillin as a primary component of vanilla bean extract, and as a crosslinking agent for entangling chitosan–PVA hydrogels. This involves a Schiff-base reaction, where amino group of chitosan (CH) interacts with aldehyde group of vanillin (Van). The optimized formula of formed hydrogels is chosen based on achieving a well-balanced combination of self-healing capability, mechanical strength, sustained release profile, and hydrophilic tendency. The prepared hydrogel is thoroughly characterized using SEM and FTIR analyses, swelling ratio, hydrolytic rate assessment, and *in vitro* drug release profiling. CH–PVA–Van hydrogels demonstrate controlled drug release that is sustained for over 7 days. Furthermore, antimicrobial tests indicate strong activity of CH–PVA–Van–L-arginine against Gram-positive bacteria, compared to tested yeast or Gram-negative bacteria using multiple human pathogens. Subsequently, *in vitro* biological assays are conducted to confirm the effectiveness of the prepared hydrogel in promoting wound healing and bone regeneration through cytotoxicity assay and wound scratch assay. The composite hydrogels achieved 95% wound healing after 24 hours, attributed to the release of NO from the loaded L-Arg and its essential role in the wound healing process. Consequently, CH–PVA–Van hydrogels emerge as a promising system for loading L-arginine and exhibiting potential for biomedical applications with antibacterial efficacy.

Received 17th June 2024
Accepted 24th September 2024

DOI: 10.1039/d4ra04430d

rsc.li/rsc-advances

1. Introduction

Regenerative medicine seeks to restore damaged tissues by applying the principles of biomedical applications, tissue engineering, and nanoscience-based drug delivery approaches.[1] Human cells need stimulation to grow and differentiate correctly after any damage. This stimulation may be molecular signals "growth factors", drugs, amino acids, and nucleotide fragments. In the past years, the most significant obstacles presented in bone regeneration, tissue engineering, and biomedicinal transplantation for tissue repair were related to the complex structure of the human tissues, limited availability of self-regenerating bones, and cell rejection.[2] Therefore, developing a soft material that is biodegradable, biocompatible with the damaged tissues, porous, adapts to different physiological conditions, has appropriate mechanical stress, furthermore, participates in cell growth, proliferation, and differentiation can be considered a good approach in biomedicine.[2] Self-healing scaffold hydrogel dependent on carbohydrate-based polymers has a potential and safe effect in pharmaceuticals.[3,4] Recently, the self-scaffold hydrogel has been used in biomedicinal applications in wound healing, tissue engineering, drug delivery, and biosensors.[4,5]

Chitosan (CH) is a natural cationic polysaccharide consisting of alternative chains of *N*-glucosamine and *N*-acetylglucosamine linked with β (1–4) glycosidic bonds. It has biocompatible, nontoxic, osteo-inductive ability, and biodegradable characteristics so, it has been utilized in different applications.[3,6] Furthermore, it has bioactive properties such as antifungal, antitumor, antibacterial, and antioxidant effects.[5] CH-

[a]*Polymeric and Biomaterials for Medical and Pharmaceutical Applications Research Group, Nanotechnology Research Center (NTRC), The British University in Egypt (BUE), Cairo, 11837, Egypt. E-mail: samar.salim@bue.edu.eg*

[b]*Department of Chemistry, College of Science, King Faisal University, Al-Ahsa 31982, Saudi Arabia. E-mail: ekamoun@kfu.edu.sa; Tel: +201283320302*

[c]*Polymeric Materials Research Dep., Advanced Technology and New Materials Research Institute (ATNMRI), City of Scientific Research and Technological Applications (SRTA-City), New Borg Al-Arab City 21934, Alexandria, Egypt*

[d]*Department of Pharmaceutics and Pharmaceutical Technology, Faculty of Pharmacy, The British University in Egypt (BUE), Cairo, 11837, Egypt*

[e]*Bioprocess Development Department (BID), Genetic Engineering and Biotechnology Research Institute (GEBRI), City of Scientific Research and Technological Applications (SRTA-City), New Borg Al-Arab City 21934, Alexandria, Egypt*

[f]*Department of Pharmacognosy, National Research Center (NRC), Dokki, 12622, Giza, Egypt*

† Electronic supplementary information (ESI) available. See DOI: https://doi.org/10.1039/d4ra04430d

based biomaterials have shown a promising role in tissue engineering, wound healing and bone regeneration. CH has many resemblances with glycosaminoglycans therefore, it can improve bone growth rate, and promote proliferation, adhesion, and differentiation of different cells.[6] The NH_2 groups of the CH are positively charged under normal physiological conditions[5] that facilitate the interaction with negatively charged agents (cell membrane) so, responsible for the mucoadhesion with human cells.[6,7] Polyvinyl alcohol (PVA) is widely used in industry, thus enormous amounts of PVA are manufactured yearly. Chemical and physical stability and other properties made PVA an excellent candidate for versatile medical applications. PVA is a water-soluble, nontoxic, biocompatible, and biodegradable synthetic polymer that belongs to the class of water-soluble nonionic polymer-containing a vinyl group. It is harmless and thus regarded as safe to handle, and it is also considered environmentally friendly.[8,9] Using a natural crosslinking agent is favorable for the green concept of biomaterials, the addition of an agent that causes self-gelation with chitosan is considered a safe approach to forming self-healing chitosan scaffolds.[4]

Vanillin (Van) is a 4-hydroxy-3-methoxybenzaldehyde, obtained from the bean extract of vanilla *tahitensis*, vanilla planifolia, and vanilla *pompona*.[10] It is considered a safe compound with an antimicrobial, and antioxidant effect. Vanillin is also used for other purposes such as a constituent in cosmetic and drug preparations.[11] The aldehyde groups of Van and the amino groups in CH may undergo a Schiff base reaction and form a mechanical network structure that will be responsible for the stabilization and controlled release of the drug.[4] One auspicious strategy is L-arginine scaffold-based hydrogel for biomedical applications and tissue engineering.

L-Arginine (L-Arg) is a natural amino acid with a guanidine chain that is converted to nitric oxide and ornithine at the application site. Nitric oxide has an antimicrobial effect, enhancer for epithelialization, furthermore, stimulates angiogenesis. Ornithine is a precursor for proline synthesis, which is considered a vital amino acid in collagen production.[12,13] L-Arg enhances vascular endothelial growth factor secretion, collagen synthesis, and cell surface migration. Moreover, stimulates protein synthesis by the activation of the mTORC1 pathway through the activation of the PI3K signaling pathway. Therefore, it can accelerate bone regeneration and wound healing.[12,14] Additionally, it serves as a precursor for creatine production and can increase the secretion of growth hormones thus, it plays an essential role in muscles metabolism.[15]

In this study, we have explored the incorporation of L-arginine into self-gelled CH–PVA–Van composite hydrogels, which holds promise as an innovative approach to enhance osteogenesis, wound healing and tissue repair. Also, this study focused on the design and characterization of CH–PVA–Van hydrogels containing varying concentrations of L-arginine to investigate its effect on the final targeted application, in terms of accelerating wound healing. Further, formed hydrogels were investigated for their potential antimicrobial and the entire biological efficacy.

2. Materials and methods

2.1. Materials

Chitosan (CH) (M_{wt} 100–300 kDa, DD< 90%, molar mass 161.16 g mol^{-1}) was purchased from Acros Organics, USA. Polyvinyl alcohol (PVA) (M_{wt} 35–124 kDa, molar mass 44.05 g mol^{-1} and 87–89% hydrolyzed) was obtained from Aldrich Chemistry, Germany. Vanillin (Van) (M_{wt} 152.149 g mol^{-1}) with maximum limits of impurities ~0.05% was purchased from Advent Cembio pvt, India. L-arginine (98%) (M_{wt} 174.20 g mol^{-1}) was purchased from Alfa-Aesar, Germany. All other reagents and other routine chemicals used were of analytical grade.

2.2. Fabrication of self-gelled CH–PVA–Van hydrogels

The hydrogel was fabricated according to Xu *et al.* route with slight modifications.[16] The method is summarized as follows: 5% (w/v) CH solution was prepared by dissolving CH in a 1.5% (v/v) glacial acetic acid aqueous solution at room temperature and stirred overnight to ensure the complete dissolution. While Van fast dissolved in pure ethanol with 20% (w/v). To obtain the plain CH–Van hydrogel formation, the prepared Van solution was added to CH solution with different ratios of CH : Van as (1 : 1, 1 : 2, 1 : 4, 2 : 1, 4 : 1, 1 : 8); respectively. The optimized formula of CH–Van hydrogel was (1 : 1). (10% w/v) PVA solution was prepared by dissolving PVA in deionized water at 60 °C under stirring for 4 h, to improve the swelling properties of prepared hydrogel. PVA solution was added to CH solution with a (1 : 1) ratio. The optimum formula (CH–PVA) : Van (1 : 1) was used to further incorporate L-arginine into the hydrogel mixture with different concentrations (0.125, 0.25, 0.5, 0.75, 1 wt%). L-Arginine powder was added to CH–PVA mixture and mixed well until became a homogeneous phase, then Van solution was added to CH–PVA-L-arginine mixture. All composition of hydrogel were carried out in glass test tubes for quick investigating the gelation process.

2.3. Determination of gelation time and gelation yield (%)

The gelation time is determined by observing the time required to form a complete gel immediately after adding Van.[17] To calculate the gel yield, the known weight of hydrogel was lyophilized by freeze dryer demonstrated as (W_1). Variables weight (CH and Van) is calculated and demonstrated as (W_2). The gel yield percentage was then calculated according to the given eqn (1).[17] The results were performed in triplicates.

$$\text{Gel yield } \% = \frac{W_1}{W_2} \times 100. \quad (1)$$

2.4. Characterization

2.4.1. FTIR analysis. FTIR devise (model: Bruker Vertex 70, Germany), were used to verify the chemical interaction among CH and Van at the spectrum of 4000 to 1500 cm^{-1} by introducing the transmittance mode. FTIR analysis was conducted for the plain CH and Van powder, (CH/Van) scaffold hydrogel with different concentrations, in addition (CH : PVA) : Van incorporated with different concentrations of L-Arg.

2.4.2. SEM investigation. FE-SEM (model: FS SEM, Quattro S, Thermo-Scientific, USA) was used to examine the surface morphology of the prepared CH/Van hydrogel scaffolds with different concentrations at different magnifications 1500× and 800×. SEM was obtained using a backscattered electron detector at 5.0–7.0 kV. Surface features of the *Image-Pro Plus* (Media Cybernetics, Rockville, MD, U.S.A.) were used to quantitatively measure and determine the scaffolds features.

2.5. Swelling ratio study

The swelling ratio of prepared hydrogel was determined by the concept of water uptake capacity. Typically, freshly prepared hydrogel with known weights denoted as (W_f) was put in a weighing bottle containing 15 mL of deionized water and incubated for 30 min at 37 °C. At different time intervals, the swelled hydrogel was placed on filter paper to remove the surface adhered liquid droplets, and then its weight was denoted as (W_s). The swelling ratio (%) of each sample was calculated using the given equation (eqn (2)).[18,19] The results were performed in triplicates.

$$\text{Swelling ratio } \% = \frac{W_s - W_f}{W_f} \times 100. \quad (2)$$

2.6. Hydrolytic degradation

The hydrolytic rate was conducted in deionized water at 37 °C for 20 h. Fresh hydrogel disks were allowed to swell in deionized water. After 5 min, swollen gels were separated from the swelling medium and carefully weighed (initial swelling weight) donates (M_o). The samples were re-introduced into the same container and weighed at regular time intervals until the hydrogels were completely degraded (M_t). The degradations (%) are determined according to eqn (3).[20,21] The results were performed in triplicates.

$$\text{Degradation rate } \% = \frac{M_o - M_t}{M_o} \quad (3)$$

2.7. *In vitro* release profile

In vitro release studies for 7 days are conducted in 20 mL of deionized water using a shaking water bath at 37 ± 0.2 °C at 50 ± 5 rpm. At predetermined time intervals, 3 mL of samples were withdrawn from each vial and replaced with an equal fresh volume of the release medium. The concentrations of L-Arg released are measured by a validated spectrophotometric method at 253 nm.[22]

2.8. Antimicrobial test

In antimicrobial bioassays, the prepared hydrogels were encoded as C1 (1% L-arginine), C2 (1% chitosan), C3 (1% vanillin), F1 (1% chitosan, 1% vanillin), F2 (1% chitosan, 1% vanillin, 0.125% L-arginine), F3 (1% chitosan, 1% vanillin, 0.25% L-arginine), F4 (1% chitosan, 1% vanillin, 0.5% L-arginine), F5 (1% chitosan, 1% vanillin, 0.75% L-arginine), and F6 (1% chitosan, 1% vanillin, 1% L-arginine). The antimicrobial capabilities of these hydrogels were assessed *in vitro* using a variety of antimicrobial bioassay approaches. These hydrogels were first evaluated qualitatively in both their dried and liquid states using the agar-disc-diffusion and agar-well-diffusion techniques. Second, the antimicrobial abilities of the examined hydrogels were evaluated quantitatively using biofilm inhibition and time-kill kinetics tests based on the micro-dilution method.[23]

2.8.1. Agar disc-diffusion method. Each of the evaluated human pathogens was individually inoculated into sterilized LB broth medium (0.5% peptone, 0.5% NaCl, and 0.3% yeast extract), then cultivated for 18 h at 37 °C and a rate of 200 rpm agitation. Each of the microbial cultures was then diluted using sterile LB broth medium to 2×10^6 CFU mL^{-1}, then cultured once more to achieve the initial OD at 0.6 (nearly 2 h of incubation period). Then, 100 μL of each plankton culture was uniformly swapped over each 90 mm LB agar plate using a sterile glass spreader. The hydrogels were then cut with a razor-sharp blade into slices of similar thickness. These slices were placed carefully on the agar surfaces that had been swapped with microbial cells. After that, these plates were incubated aerobically at 30 ± 2.5 °C for 18–24 h. The diameter of the inhibitory zones (the clear zone around each disc) was then measured on a milliliter scale using a ruler.[24]

2.8.2. Agar well-diffusion method. Briefly, each pathogenic lawn was generated by evenly spreading the pathogens onto an LB agar plate using a sterile cotton swab after they had grown until they matched the 0.5 McFarland turbidity requirements. The wells were drilled using a sterile cork-borer with a 6 mm diameter, and each well-received 50 μL of the tested hydrogels. Subsequently, these agar plates were incubated for 24 h at 37 °C, and a ruler was used to measure the diameter of the produced inhibitory zones.[25]

2.8.3. Biofilm inhibition assay. The broth dilution method, as approved by the National Committee for Clinical Laboratory Standards, was employed to evaluate the antimicrobial capability of the tested hydrogels.[26] In this approach, the inhibitory effects of our tested hydrogels were evaluated using a spectrophotometric examination. Basically, LB broth medium was separately inoculated with each of the tested human pathogens to reach 2×10^5 CFU mL^{-1}. In an aseptic condition, 900 μL of aqueous solutions containing planktonic microbes were treated with 100 μL of each of our hydrogels. Additionally, untreated control was then prepared using solely cultures of the tested pathogenic microbes. After that, all tubes were incubated for 24 to 48 h at 37 °C and 200 rpm. Then the resulting turbidity was measured at OD_{600} to evaluate the microbial growth. The biofilm inhibition percentages were then determined for each sample using the OD of the matching control as applied in eqn (4).[27]

$$\text{Biofilm inhibition } (\%) = \left[\frac{(OD_{control} - OD_{treated})}{OD_{control}}\right] \times 100. \quad (4)$$

2.8.4. Time-kill kinetics assay. The colony-forming unit yield per milliliter (CFU mL^{-1}) was computed in the time-kill assay applying the macro-broth dilution technique to count the resulting viable cells after treatments.[28,29] In this assay, *Staphylococcus aureus* and *Bacillus cereus* were treated with F5-

hydrogel (1% chitosan, 1% vanillin, and 0.75% L-arginine). Each of these pathogens was individually inoculated into LB broth medium tube to obtain 2×10^5 CFU mL^{-1} using a 0.5 McFarland turbidity standard.[26] First, these tubes were incubated at 37 °C with 200 rpm shaking for two hours to ensure that microbial growth was in the early logarithmic stage (exponential phase). Second, 9 mL of freshly prepared LB broth medium was used to dilute 1 mL of each of these exponentially growing microbial cultures before mixing it with 1 mL of F5-hydrogel. As a control, a growing setup free of F5-hydrogel was generated for each pathogen. These tubes were then incubated at 37 °C while being shaken at 200 rpm. Under aseptic conditions, the withdrawn sample (100 μL) was repeatedly diluted into 10-fold dilutions in sterile saline (0.9% NaCl). The final dilution was then swabbed onto LB agar plates in the amount of 100 μL. After 24 h of aerobic incubation at 37 °C, colonies on each plate were counted, and viable cells were expressed as CFU mL^{-1}. Then, the pathogens' cell viability was monitored using its logarithm at different intervals up to 96 hours of the incubation period. The percentage of growth reduction of the pathogen's cells exposed to F5-hydrogel was computed for each of the periods using its logarithm ($\log_{10}$ CFU mL^{-1}) as given in (eqn (5)). The time-kill curve was generated for each pathogen by plotting the $\log_{10}$ CFU mL^{-1} of viable microbial cells with cultivation periods (in hours). It was also established how long it would take to completely eradicate the pathogen's biofilm plus the bactericidal exposure duration, utilizing the ability of the tested hydrogel.[18,26]

$$\%\ \text{Of growth reduction} = \left[\frac{(\log_{10}\ \text{Colonies count}_{\text{Control}} - \log_{10}\text{Colonies count}_{\text{Treated}})}{}\right] \times 100. \quad (5)$$

2.9. *In vitro* biological assessments

2.9.1. DPPH assay. Being stable and free radical, the DPPH has been used in various studies to examine the free radical-scavenging activities of active ingredients and the prepared samples. The antioxidant activities of F1 (1% chitosan, 1% vanillin), F2 (1% chitosan, 1% vanillin, 0.125% L-arginine), F3 (1% chitosan, 1% vanillin, 0.25% L-arginine), F4 (1% chitosan, 1% vanillin, 0.5% L-arginine), F5 (1% chitosan, 1% vanillin, 0.75% L-arginine), and F6 (1% chitosan, 1% vanillin, 1% L-arginine), C1 (L-arginine), C2 (chitosan), C3 (vanillin) were tested compared to vitamin C (Vit C). Briefly, 195 μL of DPPH solution (200 μM in methanol) was mixed with 100 μL of each sample solution at a concentration of 100 μg mL^{-1} of hydrogels. The absorbance rate was recorded at 517 nm after shaking for 1 min and kept in darkness for 2 h of incubation. A stock solution of vitamin C was prepared (100 μg mL^{-1} methanol).[30,31]

2.9.2. Cytotoxic effect on human skin cell lines. Cell viability was measured by MTT-assay through the color reduction of mitochondrial from yellow MTT (3-(4,5-dimethylthiazol-2-yl)-2,5-diphenyl tetrazolium bromide) to purple formazan.[32]

2.9.2.1 Procedure. All the following procedures are done in a sterile area using a Laminar flow cabinet biosafety class II level (Baker, SG403INT, Sanford, ME, USA). Cells were suspended in DMEM-F12 medium human normal skin fibroblast (BJ1) was obtained from VACSERA, Egypt, (10 000 U mL^{-1} potassium penicillin, 10 000 μg mL^{-1} streptomycin sulfate and 25 μg mL^{-1} amphotericin B) and 1% L-glutamine at 37 °C under 5% CO_2; were obtained from GEBRI, SRTA-City, Egypt.

Cells were batch cultured for 10 days, then seeded at a concentration of 10^4 cells per well in fresh complete growth medium in 96-well microtiter plastic plates at 37 °C for 24 h under 5% CO_2 using a water-jacketed carbon dioxide incubator (Sheldon, TC2323, Cornelius, OR, USA). Media was aspirated, fresh medium without serum was added, and the cells were incubated either alone (negative control) or with the sample to give a final concentration of (100, 50, 25, 12.5, 6.25, 3.125, 1.78, 0.87 μg mL^{-1}). After 48 h of incubation; (CH : PVA) : Van: 0.125% L-Arg, (CH : PVA) : Van: 0.25% L-Arg, (CH : PVA) : Van: 0.5% L-Arg, (CH : PVA) : Van: 0.75% L-Arg, (CH : PVA) : Van: 1% L-Arg samples medium were aspirated, 40 μl MTT salt (2.5 μg mL^{-1}) was added to each well and incubated for further four hours at 37 °C under 5% CO_2. To stop the reaction and dissolve the formed crystals, 200 μL of 10% sodium dodecyl sulfate in deionized water was added to each well and incubated overnight at 37 °C. A positive control composed of 100 μg mL^{-1} was used as a known cytotoxic natural agent that gives 100% lethality under the same conditions.[33,34] The absorbance was then measured using a microplate multi-well reader (Bio-Rad Laboratories Inc., model 3350, Hercules, California, USA) at 595 nm and a reference wavelength of 620 nm. A statistical significance was tested between samples and negative control (cells with vehicle) using an independent *t*-test by *SPSS 11* program. DMSO is the vehicle used for the dissolution of hydrogels and its final concentration in the cells was less than 0.2%. The percentage of change in viability was calculated according to the formula: (((reading of extract/reading of negative control) − 1) × 100). A probit analysis was carried out for IC_{50} and IC_{90} determination using *SPSS 11* program.

2.9.3. *In vitro* scratch wound assay. HFB-4 cells (human normal skin cell line was obtained from VACSERA, Egypt) were grown in 24-well tissue culture plates at a density of 1×10^5 cells per well at (37 °C, 5% CO_2).[35] When cells accomplished 70–90% confluent monolayer, a scrape was conducted in a straight line with a 200 μl pipette tip on a monolayer to form a cell-free area. Cells were rinsed three times with PBS to remove cell debris. Then, the prepared hydrogel scaffolds were directly immersed in wells and kept under the mentioned conditions to permit cell migration to the medium. Cell migration and proliferation were observed after (0 and 24 h) using a fluorescence inverted microscope[35] (Axio observer 5, Carl Zeiss, Germany). Images were obtained with a digital camera (*Axiocam 512 Color*) in comparison with control cells.

2.10. Statistical study

Each experiment was applied triplicated, and all results were expressed as the mean ± standard deviation (M ± SD). To establish statistical significance, a one-way analysis of variance

(ANOVA) with Tukey's multiple comparison post hoc test was done using the *Minitab 17* software. A 95% confidence interval ($P \leq 0.05$) was used to establish statistical significance.[35]

3. Results and discussion

3.1. Preparation of L-arginine loaded-(CH : PVA)/Van composite hydrogel

Different concentrations of CH (2, 3, 4, 5 w/v %) were tested and mixed with different concentrations of Van (5, 10, 20, 30, 40 w/v %). As listed in Table 1, increasing CH concentration with higher Van concentration is responsible for the onset self-gelation within 30 seconds. Notably, increasing Van concentration causes massive crosslinking in the shortest time.[36] Then, the high crosslink density turned the hydrogels into hard substances. The equilibrium between CH and Van concentrations produces composite hydrogel with an accepted gelation time, where 5% w/v CH and 20% w/v Van cause complete self-gelation within only 3.5 min. Several amounts of hydrogel components were tested and optimized to achieve the accepted morphological self-gelled hydrogels, in terms of their porous, homogenous, and regular structure. Herein, various ratios of (CH 5% w/v : Van 20% w/v) (1 : 1, 1 : 2, 1 : 4, 1 : 8, 2 : 1, 4 : 1) were tested to select the accepted self-gelled hydrogels, as shown in Fig. 1. After that, the polymeric solution of PVA 10% (w/v) was added to CH solution with a ratio of (1 : 1) to improve the swelling properties of prepared composite hydrogels. The optimized formula of (CH : PVA) : Van loaded with different concentrations of L-Arg (0.125, 0.25, 0.5, 0.75, 1%). The optimized formula was investigated for biomedical applications.

3.2. Gelation time and gelation yield (%)

The gelation time of self-gelled hydrogels fully depends on (CH : Van) ratios, where at higher ratios of Van the gelation time is clearly reduced. Where, CH : Van hydrogels with ratios (1 : 2, 1 : 4, 1 : 8 v/v %) show gelation times 2, 1.5, and 0.5 min; respectively as illustrated in Fig. 1b. The summary of the effect of reaction variables on the formation of self-gelled hydrogels is shown in Fig. 1c. A good balance between the components provides a suitable intermolecular interaction between the bonds. While, at equal volumes of CH : Van (1 : 1) showed stabilization of all amino groups of CH with the aldehyde groups of Van with 85% gel yield.

3.3. Characterization

3.3.1. FTIR analysis. FTIR analysis for chitosan (powder), Van (powder), and (CH/Van) hydrogel is performed to confirm the formation of the Schiff-base/hydrogen bond hybrid network. Chitosan shows characteristic bands at ν 3393.3, 2897.7, and 1621.9 cm^{-1}.[37] Whereas the spectrum of C=O and OH of Van shows the absorbance peaks at ν 2239.3 cm^{-1}, 3186 cm^{-1}; respectively.[38] The reaction between chitosan (NH_2) groups and Van (C=O) groups is responsible for the formation of C=N imine (azomethine) bonds.[38,39] The imine stretching vibration for the hydrogel is detected around ν 1660 cm^{-1} according to Fig. 2A.[16] From Fig. 3A, increasing Van concentration is usually associated with the formation of wider C=N bonds so this characteristic bond can qualitatively evaluate the reaction efficiency. The hydroxylic (OH) group of Van is shifted from ν 3197 cm^{-1} to 3185 cm^{-1} which attributed to the formation of hydrogen bonds between NH_2 of chitosan and the OH of Van.[38] The hydroxyl group of chitosan is shifted from ν 3393.3 cm^{-1} to 2931.4 cm^{-1}, and its strength is reduced after interaction with Van, which might be due to the formulation of the hydrogen bond between chitosan and Van.[40] FTIR spectra of L-Arg crosslinked with (CH : PVA) : Van is presented in Fig. 2B. After introducing L-Arg into (CH : PVA) : Van, displays a broad band around ν 3258 cm^{-1}. This could be ascribed to the formation of hydrogen bonds between COOH/NH_2 groups of L-Arg and OH/CHO groups of CH/Van.[35] The appearance of the chitosan peak (small peak) in low concentrations of L-Arg (0.125, 0.25, and 0.5%) indicates a good homogeneity and dispersity of L-Arg in the polymeric mixture. The absence of the chitosan peak in a relatively high concentration of L-Arg (0.75%), indicates the saturation of all polymeric materials and good homogeneity of L-Arg. However, 1% of L-Arg was associated with the appearance of a chitosan peak indicating low homogeneity of L-Arg in the polymeric materials and accumulation of L-Arg on the surface.

Table 1 Different configurations of CH (2, 3, 4, 5) % with different concentrations of Van (5, 10, 20, 30, 40) % for optimizing the formula that achieved the acceptable/quick gelation time[a]

Vanillin (%) (w/v)	Chitosan (%) (w/v)			
	2	3	4	5
5	No hydrogel formed, only partial gelation after 1 : 30 h	No hydrogel formed, only partial gelation after 30 min	No hydrogel formed, only partial gelation after 24 min	No hydrogel formed, only partial gelation after 15 min
10	No hydrogel formed, only partial gelation after 1 : 15 h	No hydrogel formed, only partial gelation after 25 min	Complete gelation after 32 min	Complete gelation after 12 min
20	No hydrogel formed, only partial gelation after 1 h	Complete gelation after 3.5 h	Complete gelation after 4.20 min	[b]Complete gelation after 3.5 min
30	Complete gelation after 3.5 h	Complete gelation after 3 h	Complete gelation after 3.40 min	Complete gelation after 3 min
40	Complete gelation after 3 h	Complete gelation after 2.5 h	Complete gelation after 3 min	Complete gelation after 30 s

[a] All samples were prepared with the same ratios (CH/Van) (1/1). [b] The optimized formula.

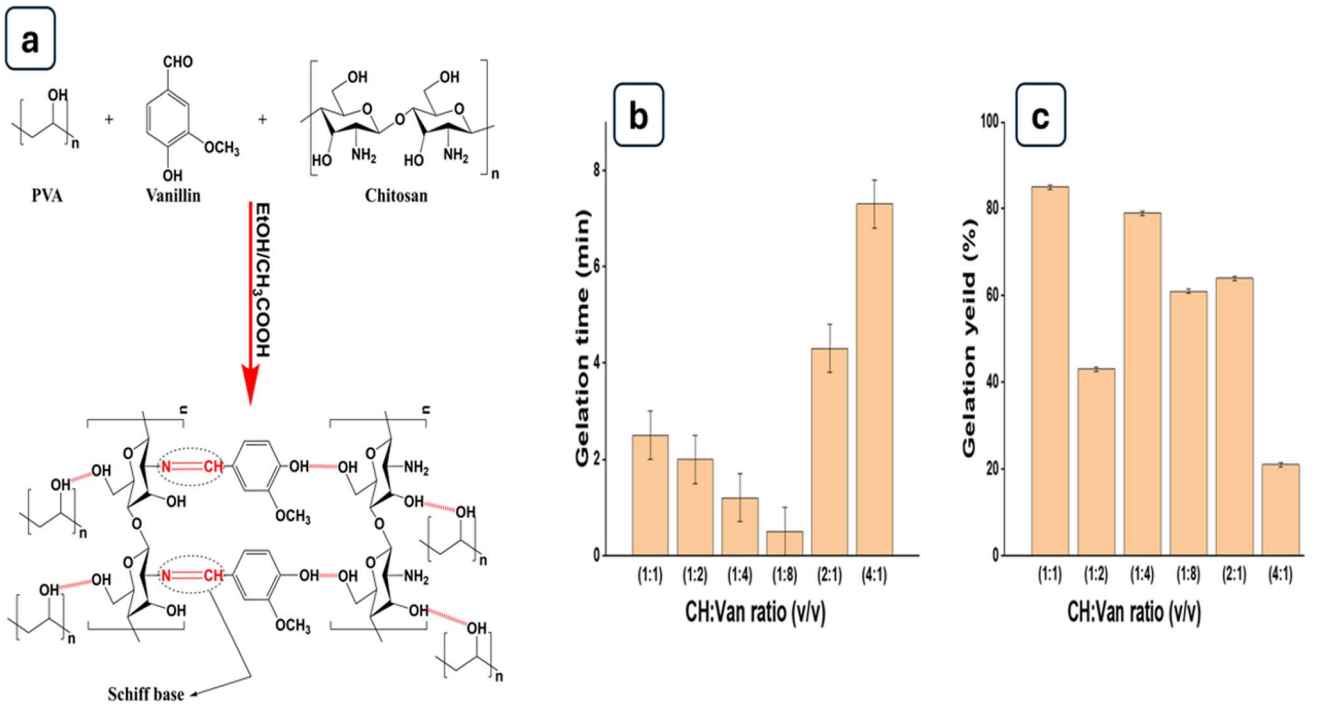

Fig. 1 The Schiff base reaction scheme for CH/PVA/Van (a) Gelation time required for hydrogel formation (b) and gelation yield (%) (c); against different ratios between Van and CH.

3.3.2. SEM investigation. SEM images indicate CH/Van composite hydrogels with different magnifications 1500× and 800×, have a three-dimensional network structure with a highly interconnected microstructure as shown in Fig. 3. Different CH/Van mass ratios are determined using SEM to obtain the optimized formula based on the regularity and the porous uniformity of self-gelled hydrogel. The formation of porous and rough structure of CH/Van hydrogel is related to the reaction between aldehyde groups of Van and amino groups of CH.[41] The presence of these porous structures in the hydrogel networks offers sufficient internal space for drug entrapment and acting as channels for drug release.[42] Interestingly, CH/Van (1 : 1) shows a homogeneous and regular porous network structure, that facilitates the transport of water and macromolecules for cell growth as illustrated in Fig. 3a. Meanwhile, increasing Van mass ratios are usually associated with irregular structure and blockage of the pours network as shown in Fig. 3b, d and e. According to the SEM image (Fig. 3c and f), increasing CH mass ratio generates surface porous and blockage of the internal networks structure.

3.4. Swelling ratio %

The swelling ratio has a significant impact on drug release from prepared hydrogel network. The swelling behavior of (CH : PVA)/Van/L-Arg hydrogels is studied by incubating at 37 °C in deionized water. The water uptake of hydrogels is relatively rapid and reached a swelling ratio value of 30% within approximately 30 min. The fast swelling of hydrogel is related to the hydrophilicity of (CH : PVA) : L-Arg with increasing the amount of L-Arg is usually associated with a higher swelling ratio as illustrated in Fig. 4a. Except for 1% L-Arg, where a high concentration of L-Arg accumulated on the surface with low homogeneity as shown in Fig. 2B. Thus, upon adding it into the water, it disperses in a high amount. So, hydrogels keep their shape and stability after long exposure to water.[43] The previous study shows that Arg-*g*-Alg hydrogels (samples were grafted with L-arginine) swelled more promptly and had a higher water uptake, compared to the neat alginate hydrogel. As the concentration of grafted L-arginine increased, the swelling ratio values increased monotonically up to 3%. This increase in swelling ratio as the L-arginine concentration went up can be attributed to the incorporation of additional hydrophilic groups like $-NH_2$ and –COOH from the L-arginine structure, which helped increase the water uptake until a certain concentration.[43]

3.5. Hydrolytic degradation rate (%)

Basically, the individual components of hydrogel, CH, PVA and Van are generally biocompatible and have lower toxicity potential at the molecular, cellular or organ level.[44] Therefore, they do not create unwanted toxic by-products after its degradation process. The time taken for the hydrogel to degrade should be designed to complement the time required for the ingrowth of new tissues. This synchronization between the hydrogel degradation and the tissue regeneration process is crucial for ensuring a successful and seamless healing or regeneration outcome.[44] The hydrolytic degradation of prepared hydrogels was described as a percentage of weight loss (%) for 1 day under incubation time after reaching the hydrogel into their equilibrium swelling state. The hydro-degradability degree of hydrogels is displayed in Fig. 4b. The chemically crosslinked

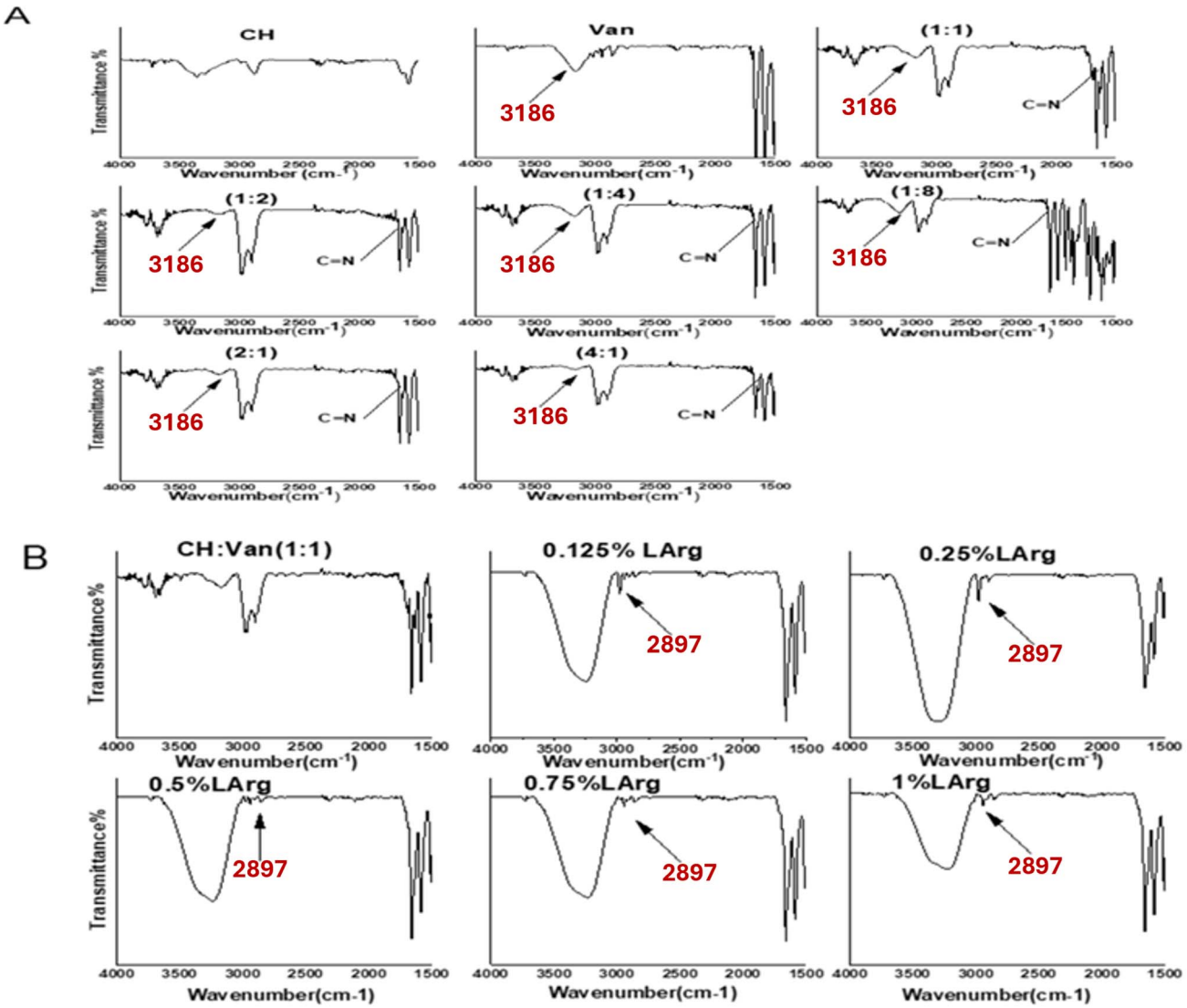

Fig. 2 FTIR spectra of different compositions of formed hydrogels; (A) (Van : CH) ratios, and (B) different L-arginine concentrations loaded hydrogels.

(CH : PVA)/Van/L-Arg hydrogels show a slow hydrolytic degradation rate. This behavior is related to using a crosslinker that forms strong crosslinking bonds between polymer chains, which improves the water resistance of hydrogel structure against hydrolytic degradation.[45] High concentrations of L-Arg (0.5, 0.75, and 1 wt/v %) show a higher degradation rate, compared to low concentrations of L-Arg (0.125 and 0.25%) as presented in Fig. 4b. This behavior is ascribed to hydrophilicity enhancement effect of L-Arg loading.[46]

3.6. Study of drug release profile

The drug release profile of (CH : PVA)/Van/L-Arg hydrogel is shown in Fig. 5. It is observed that L-Arg starts to release from hydrogels after 48 h, followed by a sustained release profile during the subsequent 7 days. It is noticed that, as the concentration of L-Arg increases, the drug release significantly enhances. This might be owing to the accumulation of drug molecules on hydrogel surface, leading to a faster drug release as known burst-effect. Additionally, the release profile depends mostly on polymer degradation and drug diffusion through Schiff base bonds.[18,47] It is worth mentioning that swelling ratio results are in good harmony with the drug release outcomes. Where, a high concentration of L-Arg is associated with higher swelling and higher drug release profile, as displayed in Fig. 1a and 5; respectively.

3.7. Antimicrobial tests

Basically, both vanillin and L-arginine have the potential to be antimicrobial agents.[27] The amount of each ingredient, the combination of items in the mixture, the concentration of the mixture, and the types of tested pathogens have an impact on how much of an inhibitory effect each ingredient when embedded in coated products.[27,48,49] Herein, varied doses of L-arginine are combined with equivalent quantities of chitosan

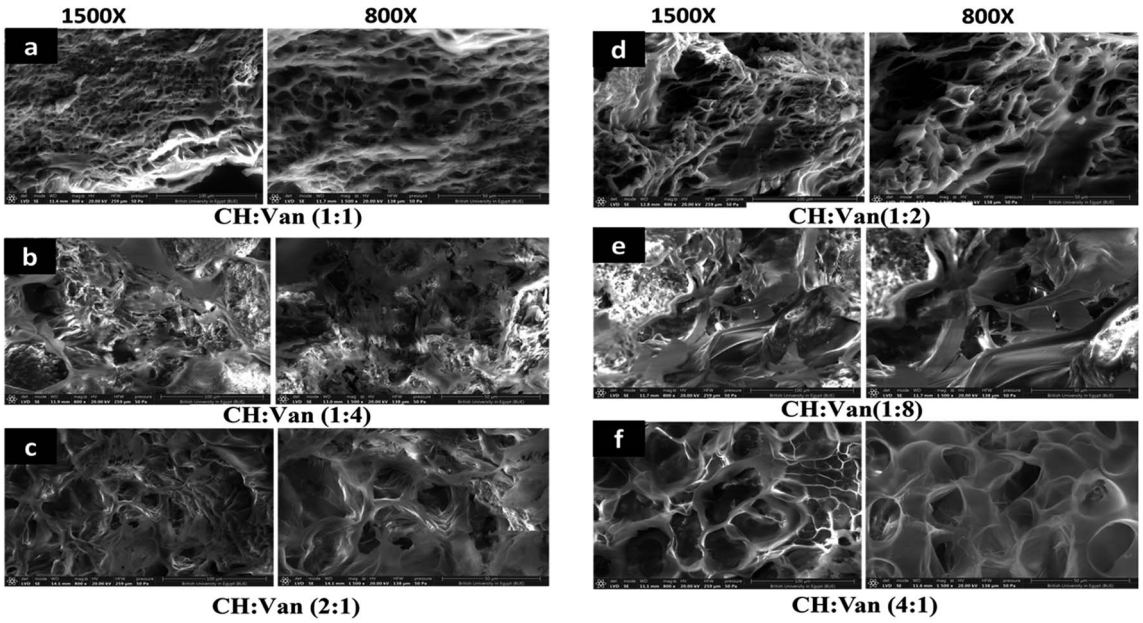

Fig. 3 SEM images of freeze-dried hydrogel of 5% (w/v) CH solution and 20% (w/v) Van solution, where hydrogels were formed with (CH : Van) mass ratios as follows: (a) (1 : 1), (b) (1 : 4), (c) (2 : 1), (d) (1 : 2), (e) (1 : 8), and (f) (4 : 1) (all images were photographed at 800× and 1500× as original magnifications and scaling 50 and 100 μm; respectively at 20 kV).

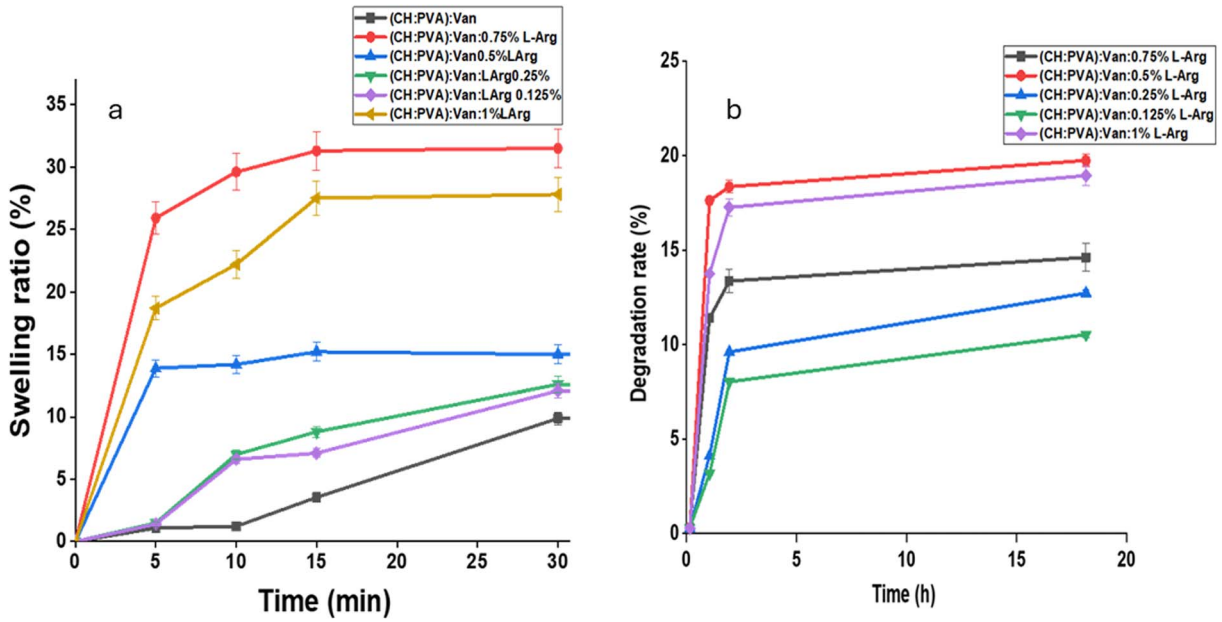

Fig. 4 Swelling ratio (%) (a), and hydrolytic degradation rate of formed CH–PVA–Van hydrogels as function of different concentrations of incorporated L-arginine (b).

and vanillin to yield six formulations, which are then tested for antimicrobial effects alongside a control group. To determine which hydrogel composition most successfully inhibits the growth of tested human pathogens, various anti-bioassay techniques can be used. To evaluate the tested hydrogel's antimicrobial properties, inhibitory halo zones are initially measured throughout agar diffusion experiments. While, the evaluated hydrogels are used in the drying and liquid phases, when conducting agar-disc and well-diffusion assays to determine their antimicrobial efficiency. According to the antimicrobial plate's photos in Fig. 6, all treatments designated as C1, C2, C3, and F1-hydrogel had negative antimicrobial effects against all tested pathogens (no inhibitory zones are detected). The investigated L-arginine, chitosan, and vanillin hydrogels generally show more potent antimicrobial activity than the L-arginine-free hydrogel (Fig. 6(i)). Particularly, F5-hydrogel (1%

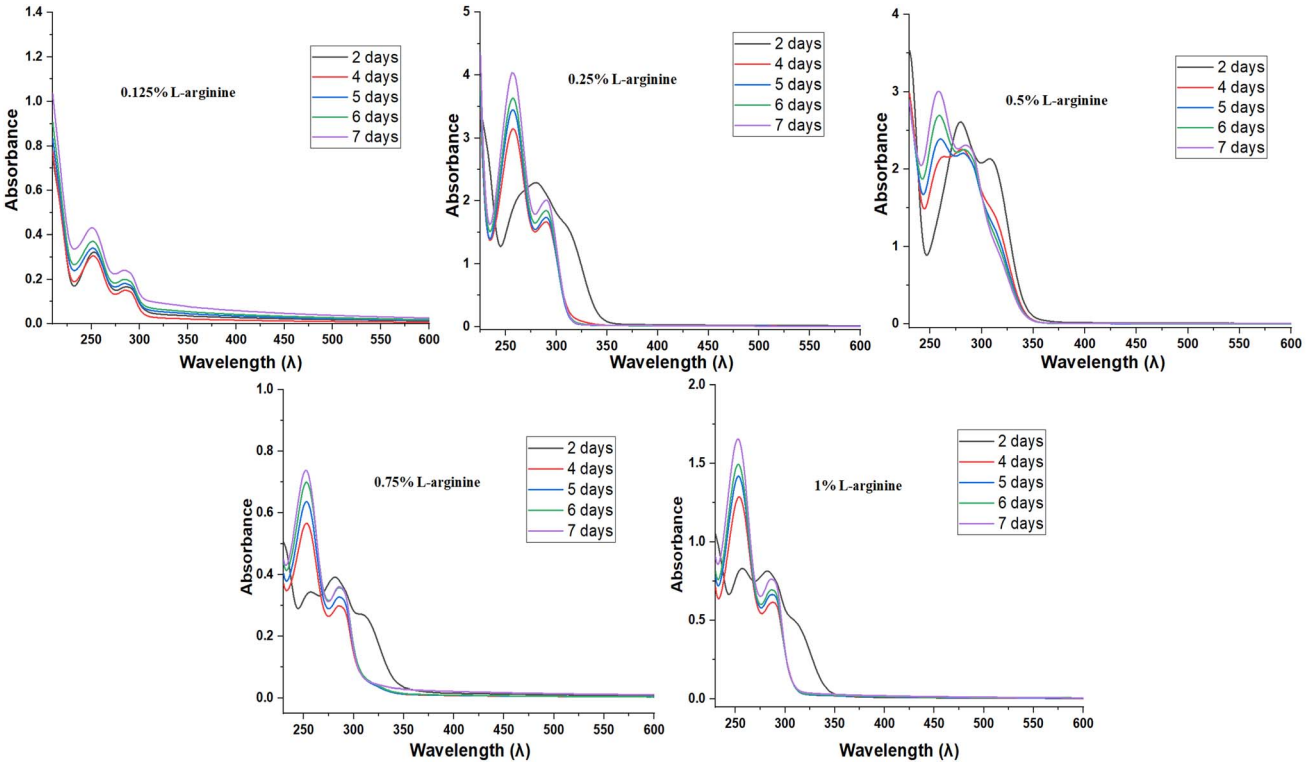

Fig. 5 *In vitro* release profiles of L-arginine from CH–PVA–Van hydrogels.

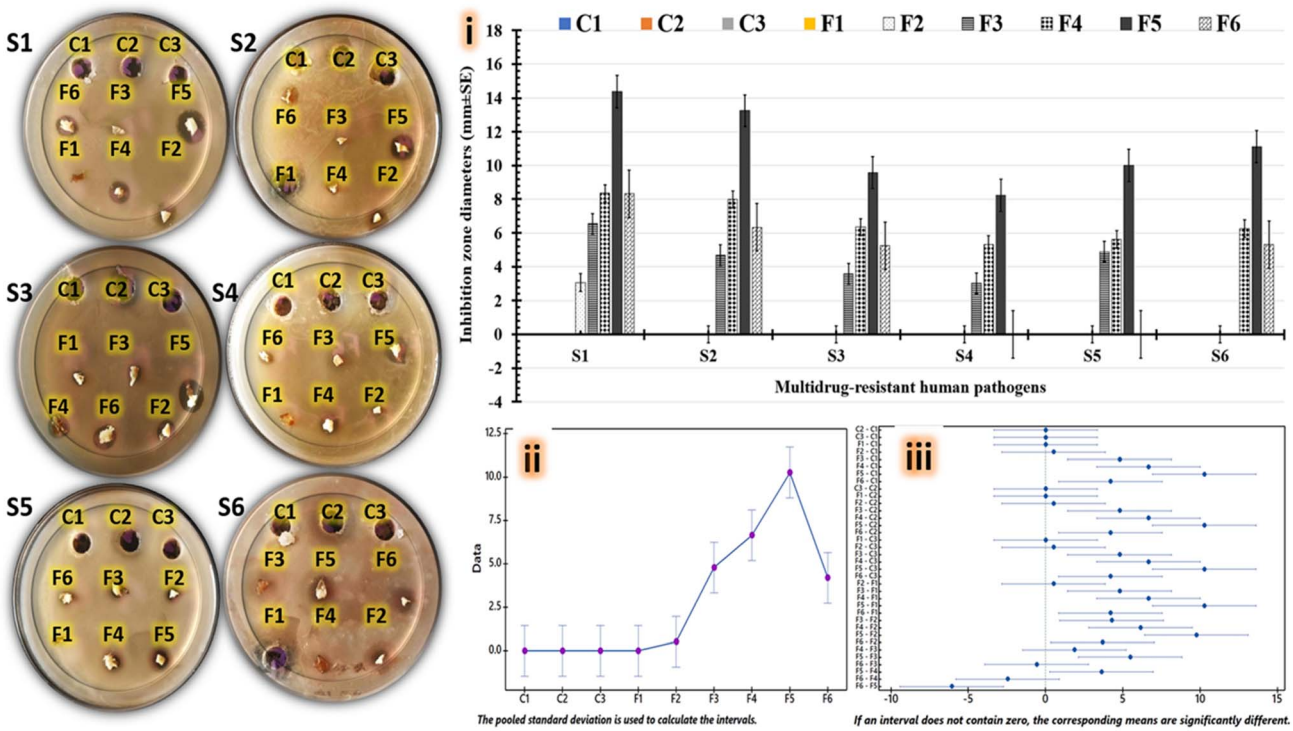

Fig. 6 Agar-disc diffusion analysis includes photographs plates, charts for calculated inhibition zones (i), interval plot (ii), and simultaneous Tukey tests for mean difference (iii) for all tested hydrogels, including: F1-hydrogel (1% chitosan, 1% vanillin, and 0% L-arginine), F2-hydrogel (1% chitosan, 1% vanillin, and 0.125% L-arginine), F3-hydrogel (1% chitosan, 1% vanillin, and 0.25% L-arginine), F4-hydrogel (1% chitosan, 1% vanillin, and 0.5% L-arginine), F5-hydrogel (1% chitosan, 1% vanillin, and 0.75% L-arginine), and F6-hydrogel (1% chitosan, 1% vanillin, and 1% L-arginine), as well as control groups including C1 (1% L-arginine), C2 (1% chitosan), and C3 (1% vanillin); that were tested against S1: *Staphylococcus aureus*, S2: *Bacillus cereus*, S3: *Salmonella paratyphi*, S4: *Escherichia coli*, S5: *Candida glabrata*, and S6: *Candida albicans*.

Table 2 Recorded inhibitory zones (in millimeters) for each evaluated hydrogel *via* Agar-disc diffusion method against several multidrug-resistant human pathogens. F1-hydrogel (1% chitosan, 1% vanillin, and 0% L-arginine), F2-hydrogel (1% chitosan, 1% vanillin, and 0.125% L-arginine), F3-hydrogel (1% chitosan, 1% vanillin, and 0.25% L-arginine), F4-hydrogel (1% chitosan, 1% vanillin, and 0.5% L-arginine), F5-hydrogel (1% chitosan, 1% vanillin, and 0.75% L-arginine), and F6-hydrogel (1% chitosan, 1% vanillin, and 1% L-arginine), as well as control groups including C1 (1% L-arginine), C2 (1% chitosan), and C3 (1% vanillin)[a]

	Inhibition zone diameters (mm ± SD)								
Multidrug-resistant human pathogens	C1	C2	C3	F1	F2	F3	F4	F5	F6
Staphylococcus aureus	ND	ND	ND	ND	3.07 ± 0.98^{c}	5.98 ± 2.35^{b}	8.36 ± 0.95^{b}	14.37 ± 2.58^{a}	8.32 ± 2.08^{b}
Bacillus cereus	ND	ND	ND	ND	ND	6.55 ± 2.47^{b}	7.99 ± 2.34^{b}	13.25 ± 1.84^{a}	6.39 ± 1.45^{b}
Salmonella paratyphi	ND	ND	ND	ND	ND	4.68 ± 1.09^{b}	6.35 ± 1.98^{b}	9.59 ± 2.14^{a}	5.24 ± 1.99^{b}
Escherichia coli	ND	ND	ND	ND	ND	3.58 ± 1.22^{b}	5.33 ± 3.24^{b}	8.23 ± 3.09^{a}	ND
Candida glabrata	ND	ND	ND	ND	ND	3.02 ± 0.97^{b}	5.62 ± 0.98^{b}	5.02 ± 0.98^{a}	ND
Candida albicans	ND	ND	ND	ND	ND	4.89 ± 0.37^{b}	6.25 ± 0.41^{b}	11.11 ± 5.47^{a}	5.31 ± 2.07^{b}

[a] ND: signifies not detected. The data is shown as the mean (millimeters) ± standard deviation (mm ± SD). The differences in the superscript letters are statistically significant at $p < 0.05$. *R*-sq (82.62%), adj *R*-sq (79.53%), and pred *R*-sq (74.97%).

chitosan, 1% vanillin, and 0.75% L-arginine) exhibit more effective antimicrobial effects, when compared to other hydrogels evaluated. The mean values of the computed antimicrobial effects are analyzed using *ANOVA* and *Tukey Post Hoc* test, as shown in Fig. 6a(ii) and (iii); respectively, to identify the more effective hydrogel statistically. In the interval plot, the mean values for C2-treatment and F5-hydrogel have been identified as the lowest and the highest values; respectively Fig. 6a(ii). The adjusted confidence intervals are computed using *Tukey* simultaneous tests above 95% scale. Our *Tukey* graph Fig. 6(iii) reveals that F5-hydrogel intervals do not include a zero line. Also, F5-hydrogel differs in significant ways that is statistically significant, compared to control group and other tested hydrogels. The conclusive results show that tested F5-hydrogel exhibits statistically significant antimicrobial properties (Table 2).

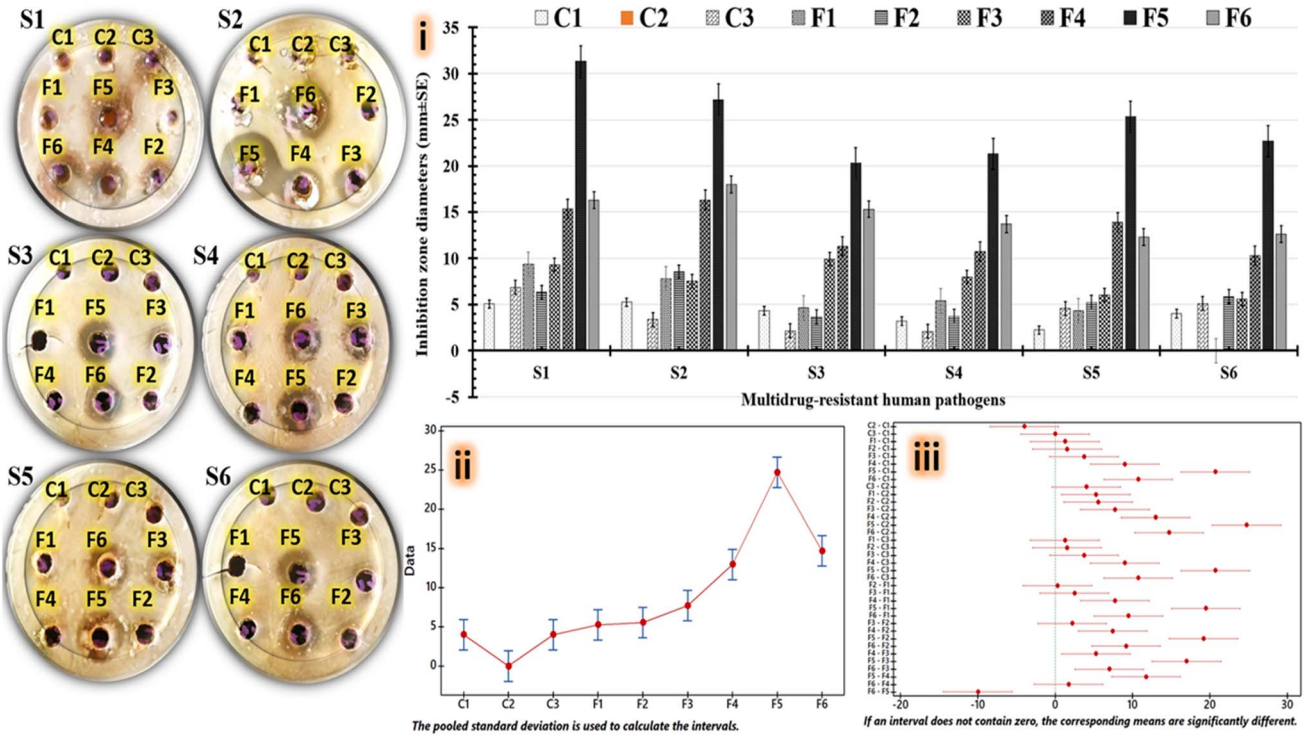

Fig. 7 Agar-well diffusion analysis consisting of photographs of antimicrobial plates, inhibition zone charts (i), interval plot (ii), and simultaneous Tukey tests for mean difference (iii) for tested hydrogels against S1: *Staphylococcus aureus*, S2: *Bacillus cereus*, S3: *Salmonella paratyphi*, S4: *Escherichia coli*, S5: *Candida glabrata*, and S6: *Candida albicans*. The tested hydrogels coded as F1-hydrogel (1% chitosan, 1% vanillin, and 0% L-arginine), F2-hydrogel (1% chitosan, 1% vanillin, and 0.125% L-arginine), F3-hydrogel (1% chitosan, 1% vanillin, and 0.25% L-arginine), F4-hydrogel (1% chitosan, 1% vanillin, and 0.5% L-arginine), F5-hydrogel (1% chitosan, 1% vanillin, and 0.75% L-arginine), and F6-hydrogel (1% chitosan, 1% vanillin, and 1% L-arginine), with a control group; C1 (1% L-arginine), C2 (1% chitosan), and C3 (1% vanillin).

Table 3 Recorded inhibitory zones for each generated hydrogel that evaluated against several multidrug-resistant human pathogens *via* Agar-well diffusion assay. F1-hydrogel (1% chitosan, 1% vanillin, and 0% L-arginine), F2-hydrogel (1% chitosan, 1% vanillin, and 0.125% L-arginine), F3-hydrogel (1% chitosan, 1% vanillin, and 0.25% L-arginine), F4-hydrogel (1% chitosan, 1% vanillin, and 0.5% L-arginine), F5-hydrogel (1% chitosan, 1% vanillin, and 0.75% L-arginine), and F6-hydrogel (1% chitosan, 1% vanillin, and 1% L-arginine), in addition control group including C1 (1% L-arginine), C2 (1% chitosan), and C3 (1% vanillin)[a]

Multidrug-resistant human pathogens	Inhibition zone diameters (mm ± SD)								
	C1	C2	C3	F1	F2	F3	F4	F5	F6
Staphylococcus aureus	5.05 ± 0.57^{cd}	ND	6.85 ± 0.97^{cd}	2.34 ± 0.98^{c}	8.38 ± 3.45^{c}	9.32 ± 3.78^{c}	15.32 ± 1.74^{b}	31.32 ± 3.87^{a}	16.31 ± 2.22^{b}
Bacillus cereus	5.24 ± 1.25^{cd}	ND	3.35 ± 0.22^{cd}	1.82 ± 1.11^{c}	8.59 ± 2.09^{c}	7.55 ± 0.97^{c}	16.32 ± 5.14^{b}	27.29 ± 1.09^{a}	17.99 ± 4.19^{b}
Salmonella paratyphi	4.35 ± 1.87^{cd}	ND	2.13 ± 0.65^{cd}	3.54 ± 2.84^{c}	4.61 ± 1.08^{c}	9.93 ± 2.09^{c}	11.88 ± 1.98^{b}	20.31 ± 3.12^{a}	15.31 ± 1.07^{b}
Escherichia coli	3.21 ± 0.09^{cd}	ND	2.09 ± 0.54^{cd}	1.72 ± 0.99^{c}	5.39 ± 0.99^{c}	7.98 ± 2.87^{c}	10.72 ± 2.22^{b}	21.92 ± 5.21^{a}	13.72 ± 4.55^{b}
Candida glabrata	2.22 ± 1.54^{cd}	ND	4.56 ± 0.34^{cd}	1.34 ± 0.22^{c}	5.22 ± 1.45^{c}	6.03 ± 0.97^{c}	13.89 ± 4.57^{b}	25.37 ± 5.82^{a}	12.32 ± 1.54^{b}
Candida albicans	3.99 ± 2.09^{cd}	ND	5.09 ± 0.89^{cd}	ND	5.58 ± 1.85^{c}	5.85 ± 0.98^{c}	10.31 ± 3.21^{b}	22.72 ± 4.04^{a}	12.65 ± 1.41^{b}

[a] ND: signifies not detected. The data is shown as the mean (millimeters) ± standard deviation (mm ± SD). The different superscript letters are statistically significant at $p < 0.05$. *R*-sq (91.58%), adj *R*-sq (90.09%), and pred *R*-sq (87.88%).

According to Fig. 7, the inhibitory zones of all aqueous hydrogels were evaluated accurately using an agar-well diffusion experiment. As shown in images of antimicrobial plates, tested F5-hydrogel's inhibitory zones against all tested human diseases are still generally greater than those of other tested hydrogels. Fig. 7(i) shows that C2 treatment containing 1% chitosan, failed to produce inhibitory zones against all examined human pathogens. This result is in line with a previous study that showed the tested chitosan films lacked any antibacterial activity against human pathogens.[50] The reason for the ineffective antibacterial outcomes might be the chitosanase enzyme, which is produced by some human pathogens, hydrolyzing the chitosan in these studied films.[51,52] According to the interval plot Fig. 7(ii), C2 and F5 hydrogels record the lowest and the highest mean values of the inhibitory zones that developed. There is a statistically significant difference between F5-hydrogel and other tested hydrogels because the intervals for F5-hydrogel display distant areas from the zero line, as shown in Fig. 7(iii) F5-hydrogel has a distinct superscript letter, compared to other hydrogels under examination which makes its mean inhibitory zone values statistically significant, as seen in Table 3. Additionally, the differences between F6 and F4 hydrogels are not statistically significant because they share the same superscript letter. The largest F5-hydrogel-inhibitory zones are detected in Gram-positive bacteria such as *Staphylococcus aureus* (31.32 ± 3.87 mm) and *Bacillus cereus* (27.29 ± 1.09 mm), which are followed by yeast cells *Candida glabrata* (25.37 ± 5.82 mm) and then *Candida albicans* (22.72 ± 4.04 mm). Furthermore, the smallest F5-hydrogel-inhibitory zones are detected against *Salmonella paratyphi* (20.31 ± 3.12 mm) and *Escherichia coli* (21.92 ± 5.21 mm) as Gram-negative bacteria (Table 3).

Biofilm inhibition (%) is calculated after different human pathogens which are exposed to composite hydrogels (Fig. 1S, ESI info.†). All tested hydrogels have different superscript letters, which make their mean percentage of biofilm reduction values statistically significant, as seen in Table 4. According to the charts in (Fig. 1S(i), ESI info.†), F5-hydrogel followed by F6-hydrogels produce the highest percentage of biofilm reduction, when tested against all the observed pathogens. Additionally, a moderate percentage of biofilm reduction is recorded in the

Table 4 Percentages of biofilm inhibition for each hydrogel evaluated against several multidrug-resistant human pathogens. F1-hydrogel (1% chitosan, 1% vanillin, and 0% L-arginine), F2-hydrogel (1% chitosan, 1% vanillin, and 0.125% L-arginine), F3-hydrogel (1% chitosan, 1% vanillin, and 0.25% L-arginine), F4-hydrogel (1% chitosan, 1% vanillin, and 0.5% L-arginine), F5-hydrogel (1% chitosan, 1% vanillin, and 0.75% L-arginine), and F6-hydrogel (1% chitosan, 1% vanillin, and 1% L-arginine), in addition control group including C1 (1% L-arginine), C2 (1% chitosan), and C3 (1% vanillin)

Multidrug-resistant human pathogens	Biofilm inhibition (% ± SD)								
	C1	C2	C3	F1	F2	F3	F4	F5	F6
Staphylococcus aureus	51.57 ± 4.83^{de}	2.03 ± 0.09^{f}	42.36 ± 5.68^{e}	52.81 ± 6.17^{cde}	65.61 ± 4.97^{bcd}	67.50 ± 6.11^{bc}	72.36 ± 2.31^{ab}	95.09 ± 2.21^{a}	90.75 ± 3.66^{a}
Bacillus cereus	49.09 ± 2.97^{de}	3.65 ± 0.97^{f}	42.36 ± 3.45^{e}	55.81 ± 8.88^{cde}	63.12 ± 2.99^{bcd}	69.78 ± 2.97^{bc}	74.32 ± 3.97^{ab}	96.55 ± 3.24^{a}	92.05 ± 7.97^{a}
Salmonella paratyphi	39.45 ± 4.98^{de}	5.24 ± 1.85^{f}	35.47 ± 2.11^{e}	42.09 ± 5.87^{cde}	48.66 ± 1.16^{bcd}	51.19 ± 6.17^{bc}	68.66 ± 1.41^{ab}	75.84 ± 3.09^{a}	70.97 ± 2.06^{a}
Escherichia coli	38.52 ± 8.89^{de}	6.48 ± 2.09^{f}	36.21 ± 3.71^{e}	41.45 ± 1.28^{cde}	42.78 ± 2.98^{bcd}	47.32 ± 6.45^{bc}	65.12 ± 3.22^{ab}	73.02 ± 2.97^{a}	70.82 ± 6.17^{a}
Candida glabrata	42.81 ± 3.98^{de}	3.21 ± 0.89^{f}	48.65 ± 2.94^{e}	60.98 ± 6.54^{cde}	55.68 ± 6.37^{bcd}	65.61 ± 4.97^{bc}	67.01 ± 6.54^{ab}	77.50 ± 6.11^{a}	69.28 ± 7.87^{a}
Candida albicans	46.53 ± 8.46^{de}	3.87 ± 2.04^{f}	39.12 ± 6.33^{e}	52.75 ± 6.97^{cde}	60.24 ± 2.18^{bcd}	66.15 ± 2.91^{bc}	64.05 ± 8.61^{ab}	79.29 ± 5.93^{a}	71.12 ± 2.92^{a}

cases of F3, and F4 hydrogels. The C2 treatment and F5-hydrogel are located to have the lowest and highest mean anti-biofilm percentage values; respectively, as displayed in the interval map plot (Fig. 1S(ii) ESI info.†). The simultaneous confidence level is then set at 95% for the Tukey analysis to determine the individual confidence level for each group (Fig. 1S(iii), ESI info.†). The difference between the means of F5-hydrogel groups and control groups is statistically significant, as demonstrated in (Fig. 1S(iii) ESI info.†), because the confidence intervals for their differences do not include a zero line. As shown in (Fig. 1S(i), ESI info.†), the reported biofilm inhibition percentages for all tested hydrogels against the treated Gram-negative bacteria and yeast cells are significantly lower when compared to Gram-positive bacteria. Also, F5-treated Gram-negative microbes show the lowest percentage of biofilm inhibition, with an average of 73.02 ± 2.97% for *Escherichia coli* and 75.84 ± 3.09% for *Salmonella paratyphi*. According to Table 4, F5-treated *Candida albicans* and *Candida glabrata* have biofilm inhibition percentages of 79.29 ± 5.93% and 77.50 ± 6.11%; respectively, which are slightly close to those seen against Gram-negative bacteria. As listed in Table 4, F5-treated Gram-positive bacteria shows the most drastic drop in the generated biomass quantities, with *Bacillus cereus* reporting anti-biofilm reduction of 96.55 ± 7.24% and *Staphylococcus aureus* indicative of 95.09 ± 6.21%.

To further explore the antimicrobial characteristics of F5-hydrogel, the time-kill kinetics for the treated Gram-positive bacteria are investigated. The reported findings of time-kill kinetics are collected and presented in Table 5 and (Fig. 2S, ESI info.†). The tested F5-hydrogel successfully lowers the planktonic viable counts of *Staphylococcus aureus* (Fig. 2SA, ESI info.†) and *Bacillus cereus* (Fig. 2SB, ESI info.†), compared to their controls. Notably, F5-treated *Bacillus cereus* cells lost considerably more planktonic viable counts over cultivation periods than F5-treated *Staphylococcus aureus* cells. The stacked bar graph (Fig. 2SC, ESI info.†) demonstrates that tested F5-hydrogel successfully decreases the pathogens' percentage of planktonic viability as compared to untreated cells (controls). After 24 hours of inoculation with tested F5-hydrogel, the percentage of viable counts ($\log_{10}$ CFU mL^{-1}) of tested *Staphylococcus aureus* and *Bacillus cereus* are reduced to 3.3 and 2.4%; respectively, compared to their controls. The growth reduction percentages in treated pathogens improve with the length of the culturing period, as shown in (Fig. 2SD, ESI info.†). After 12 hours of the pathogen being incubated with F5-hydrogel, the growth reduction percentages of *Staphylococcus aureus* and *Bacillus cereus* increases to 84.98 ± 4.89 and 87.47 ± 2.08%; respectively (Table 5). The reduction percentages of F5-treated *Staphylococcus aureus* and *Bacillus cereus* increases significantly further to 96.69 ± 2.69 and 97.59 ± 1.86%, respectively; after the incubation time to 24 h.

The bactericidal time (99.9% killing) proves to be the critical period for tested antimicrobial agent that would lower the initial inoculum by >3 $\log_{10}$ CFU mL^{-1}.[53] Herein, the bactericidal time required to inhibit F5-treated *Staphylococcus aureus* and *Bacillus cereus* biofilms by >0.52, and 0.38 $\log_{10}$ CFU mL; respectively, is determined after 36 h of cultivation period. While the time-kill kinetics experiment is also used to estimate the duration of F5-hydrogel treatment required to completely eradicate the pathogens' biofilm. Also, F5-treated *Staphylococcus aureus* and *Bacillus cereus* biofilms are destroyed (zero CFU mL^{-1}) after 96 and 72 h; respectively. Finally, it was observed that tested F5-hydrogel is more efficient against Gram-positive bacteria than against yeast cells and Gram-negative bacteria. Therefore, it is shown that F5-hydrogel (1% chitosan, 1% vanillin, and 0.75% L-arginine) offers strong antimicrobial properties. Accordingly, it might be an ideal choice for an eco-friendly, promising antimicrobial agent used to inhibit the growth of a variety of human pathogens. The research conducted by Iftime and coworkers[54] demonstrated the antifungal capabilities of the CH–Van hydrogel. Their findings revealed that the hydrogel exhibited the highest antifungal activity against *Candida albicans*, with an inhibition zone of 66 mm. The hydrogels also displayed strong antifungal activity against *Penicillium chrysogenum*, with an inhibition zone of around 40 mm. Furthermore, the hydrogels showed good activity against *Candida glabrata* and *Cladosporium cladosporioides*, both exhibiting inhibition zones of approximately 20 mm. Notably, the hydrogels did not exhibit any inhibition zones against *Staphylococcus aureus*, *Escherichia coli*, and *Enterococcus faecalis*.[54] Due to their inhibitory effects on pathogens brought on by cell wall destruction and considerable changes in gene

Table 5 *In vitro* time-kill kinetics of F5-treated *Staphylococcus aureus*, and *Bacillus cereus* with their untreated controls

	Multidrug-resistant human pathogens treated with F5-hydrogel (1% chitosan, 1% vanillin, 0.75% L-arginine)					
	Staphylococcus aureus			*Bacillus cereus*		
Incubation period (h)	Cell viability ($\log_{10}$ CFU ml^{-1} ± SD)		% of growth reduction (% ± SD)	Cell viability ($\log_{10}$ CFU ml^{-1} ± SD)		% of growth reduction (% ± SD)
	Control	Treated		Control	Treated	
0	2.71 ± 0.63	2.69 ± 0.19	0.95 ± 0.19	4.31 ± 0.38	4.30 ± 1.02	0.29 ± 0.07
6	8.29 ± 0.76	2.39 ± 0.51	71.19 ± 2.62	7.24 ± 0.39	1.39 ± 0.79	80.70 ± 2.95
12	11.31 ± 1.75	1.69 ± 0.89	84.98 ± 4.89	8.31 ± 1.75	1.04 ± 0.13	87.47 ± 2.08
18	10.32 ± 2.19	0.97 ± 0.07	90.53 ± 1.79	8.45 ± 0.48	0.27 ± 0.08	96.70 ± 3.03
24	8.41 ± 1.68	0.27 ± 0.08	96.69 ± 2.69	7.31 ± 1.95	0.17 ± 0.06	97.59 ± 1.86

expression, vanillin, and L-arginine have previously been recognized as extremely promising antimicrobial agents.[55–58]

The composite of PVA/CH/Van hydrogel has been previously fabricated, and its antimicrobial properties were investigated.[36] This study prepared different hydrogel composites with varying concentrations of Van (1.3%, 1.5%, and 1.7%) and tested their efficacy against *E. coli* and *S. aureus* over a 24 hours period. The results showed that increasing the Van concentration enhanced the antibacterial properties of the hydrogels. Specifically, the hydrogel composite with (3% CH/9% PVA/1.7% Van) exhibited inhibition zones of 6 mm and 5.8 mm against *E. coli* and *S. aureus*, respectively. In comparison, the optimized hydrogel fabricated in the current study, with a composition of (CH : PVA) : Van: 0.75% L-Arg, demonstrated larger inhibition zones of 8 mm against *E. coli* and 14.5 mm against *S. aureus*. These observations clearly indicate that the optimized hydrogel formulation has superior antibacterial properties compared to the previously reported PVA/CH/Van hydrogels. Moreover, the addition of L-Arg enhances the cell migration to reach wound healing (%) of 95% after 24 h. In conclusion, the comparison between the previous PVA/CH/Van hydrogel study and the current optimized hydrogel formulation reveals significant improvements in antibacterial and wound healing properties.

3.8. *In vitro* biological assessments

3.8.1. DPPH assay. The % of DPPH scavenging activities of samples codes F1, F2, F3, F4, F5, and F6 are found of 33.2, 35.1, 38.4, 39.2, 45.0, and 51.2%; respectively, while for the same concentrations of free L-Arg, CH and Van are found of 11.5, 3.8, and 13.5%; respectively. Vitamin C exhibits a scavenging activity of 12 ± 3.5% at the same concentrations. The scavenging activity varied significantly among different formulations and pure components, as shown in Fig. 8a. At the concentration of 100 μg mL^{-1}, while all formulated composite hydrogels have an antioxidant effect, compared to L-Arg, CH, and Van alone.[36] From Fig. 8a, there is a significant difference between Vit C, F5, and F6 of 12, 45, and 51.2%; respectively. Where high concentrations of L-Arg (F5 and F6) are associated with higher antioxidant effects, compared to others. Hence, L-Arg improves the antioxidant properties of CH/PVA/Van hydrogel in a dose-dependent manner.

3.8.2. Cytotoxicity test. The cytotoxic effect of the prepared composite hydrogels on the *BJ1* normal cell line was evaluated through the MTT assay,[56] and the results are drawn in Fig. 8b. The primary screening was performed at 100% concentration, and the results above 75% underwent secondary screening to calculate IC_{50} values. According to Fig. 8b, when the cells were treated with a concentration of 100 μg mL^{-1} of each hydrogel, the highest toxicity percentage (91.2% ± 3.05) was observed for the hydrogel containing the highest concentration of L-Arg (1%), which also displayed the lowest IC_{50} of 45.6 μg mL^{-1}. In contrast, the lower concentrations of L-Arg (0.125, 0.25, 0.5, and 0.75 wt/v %) were associated with lower cytotoxic effects (61.4 ± 2.01, 60.8 ± 0.92, 66.6 ± 1.984, and 67.1 ± 2.097; respectively) and higher IC_{50} values (85, 86, 81, and 80 μg mL; respectively). The results reveal that when the normal cells were treated with 50 μg mL^{-1} of each hydrogel, all formulations were found to be safe for the cells, except the hydrogel loaded with 1% L-Arg, which recorded a 68% cell mortality rate. Based on the IC_{50} values of the optimized formulas (CH : PVA : Van: 0.75 L-Arg and CH : PVA : Van: 0.5 L-Arg), the optimal concentrations that will be suitable for use as a dressing material is approximately 80 μg mL^{-1}.

3.8.3. *In vitro* wound scratch assay. A wound assay was conducted on *HFB-4* cells to estimate the migration and proliferation profile of composite hydrogels. Fig. 9 illustrates the kinetics of wound healing process and wound closure efficiency of prepared hydrogels after incubation of 24 h. In general, all tested hydrogels accelerate the rate of gap closure (%) after 24 h, compared to negative control as seen in Fig. 9a. According to Fig. 9e and f, hydrogels accelerate the rate of gap-closure significantly when the concentration of L-Arg is high,

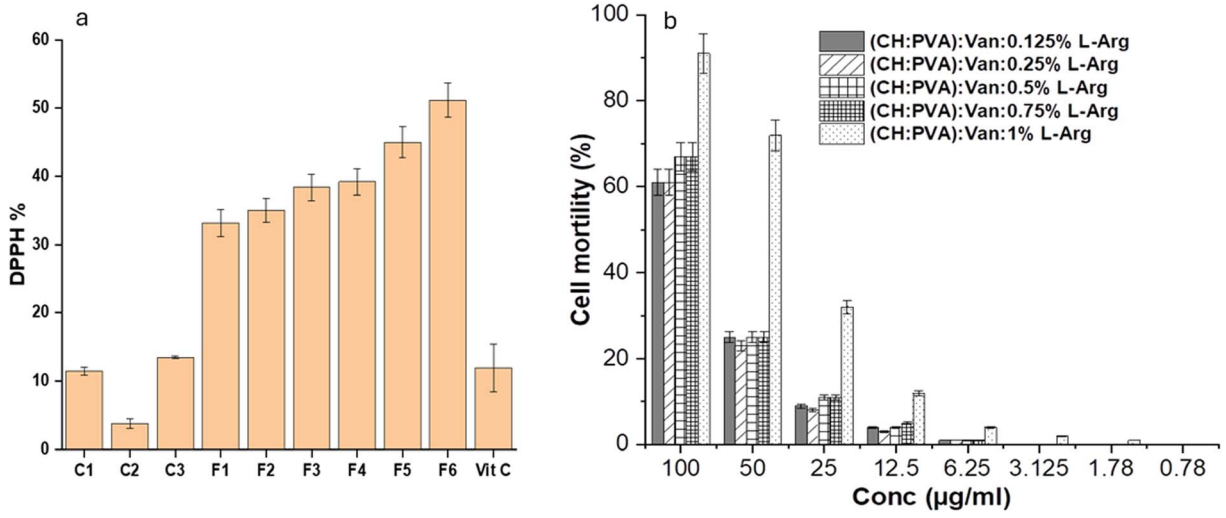

Fig. 8 (a) Percentage of DPPH of different CH–PVA–Van hydrogels loaded with different concentrations of L-Arg compared with pure components. (b) Cytotoxic activity of the prepared CH–PVA–Van–L-arginine hydrogels on the normal cell lines (BJ1).

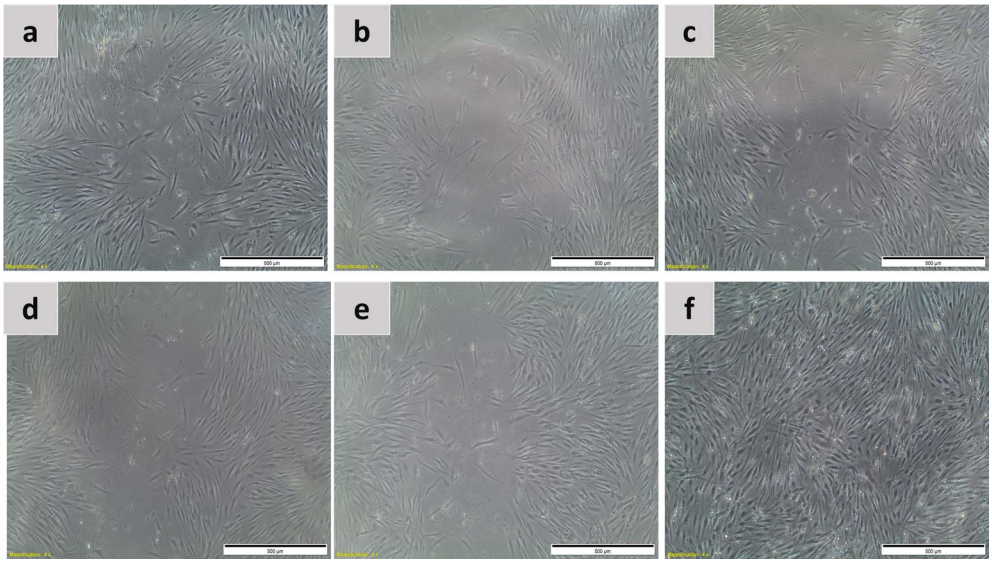

Fig. 9 Scratch wound assay (a) (negative control), (b) (CH : PVA) : Van: 0.125% L-Arg, (c) (CH : PVA)Van: 0.25% L-Arg, (d) (CH : PVA) : Van: 0.5% L-Arg, (e) (CH : PVA) : Van: 0.75% L-Arg (f) (CH : PVA) : Van: 1% L-Arg of hydrogel scaffolds using concentrations 1.5 mg mL^{-1} after 24 h of incubation time (all images were taken with scale bar 500 μm).

due to the stimulatory effect of L-Arg for epithelial cells migration and differentiation. Notably, (CH : PVA)/Van/L-Arg scaffolds hydrogel offered a prominent wound healing effect that increases by increasing the concentration of examined hydrogel. (CH : PVA)/Van/1% L-Arg composite hydrogels reach wound healing (%) of 95% after 24 h. This amazing result is owing to releasing of NO from the loaded L-Arg. As aforementioned, NO molecule is essential for the four phases of the wound healing process, besides the vital role of L-Arg for collagen synthesis and proliferation.[18,56–58] Where an increase in L-Arg concentration is usually associated with a higher migration rate.[12,14]

4. Conclusions

Self-gelled L-Arg loaded-CH/PVA/Van composite hydrogels were successfully prepared based on the green-synthesis concept of Van as a natural crosslinking agent. The reversible hybrid linkage in hydrogel network included Schiff-base and physical hydrogen bonds. The concentration of Van was critical to the self-gelation process capability of CH hydrogel. Lower Van concentration produced a weak and tacky hydrogel without any practical application values, while higher Van concentration resulted in a strong polymeric matrix without any self-healing behavior. It was found that, 0.5 mL 5% (w/v) CH solution and 0.5 mL of 10% (w/v) PVA was professionally self-gelled with 1 mL of 20% (w/v) Van and 0.75% of L-Arg, and achieved a good balance between self-healing ability and mechanical strength, and reaching a moderate gelation time of 2.30 min. *In vitro* drug release capacities of hydrogels were improved depending on the L-Arg amount in the hydrogel matrix, owing to the higher swelling capacity of the drug. L-arginine was loaded into hydrogel with different concentrations and showed high efficacy against several human pathogens. *In vitro* biological assays were performed for the prepared hydrogels and showed excellent efficacy for offering promising biomaterials could be self-gelled for versatile biomedical applications such as bone, cartilage regeneration and wound healing.

Data availability

The datasets used and analyzed during the current study are available from the corresponding author on reasonable request.

Author contributions

Rabab Ibrahim: experiments, data acquisition, interpretation of data, data analysis and wrote the original draft; E. A. Kamoun: design of the work, draft revision, supervision, revised the final draft. Noha Badawi: conception, data analysis, draft revision, supervision; S. H. El-Moslamy: experiments and drafting microbiology part; Mahmoud kh.: experiments of cell culture parts and Samar Salim: data analysis, draft revision, supervision, revised the final draft. All authors have approved the manuscript before submission. All authors have critically reviewed and approved the final draft and are responsible for the content and similarity index of the manuscript.

Conflicts of interest

The authors declare that they have no competing interests.

References

1 S. Taokaew, W. Kaewkong and W. Kriangkrai, Recent Development of Functional Chitosan-Based Hydrogels for Pharmaceutical and Biomedical Applications, *Gels*, 2023, **9**, 277, DOI: 10.3390/GELS9040277.

2 V. Chimisso, M. A. Garcia and S. Y. Avsar, Design of bio-conjugated hydrogels for regenerative medicine applications: from polymer scaffold to biomolecule choice, *Molecules*, 2020, **25**(18), 4090, **https://www.mdpi.com/1420-3049/25/18/4090**.

3 N. Salahuddin, S. Awad and M. Elfiky, Vanillin-crosslinked chitosan/ZnO nanocomposites as a drug delivery system for 5-fluorouracil: study on the release behavior *via* mesoporous ZrO2-Co3O4 nanoparticles modified sensor and antitumor activity, *RSC Adv.*, 2022, **12**, 21422–21439, DOI: **10.1039/d2ra02717h**.

4 C. Xu, W. Zhan, X. Tang, F. Mo, L. Fu and B. Lin, Self-healing chitosan/vanillin hydrogels based on Schiff-base bond/hydrogen bond hybrid linkages, *Polym. Test.*, 2018, **66**, 155–163, DOI: **10.1016/j.polymertesting.2018.01.016**.

5 R. Parhi, Drug delivery applications of chitin and chitosan: a review, *Environ. Chem. Lett.*, 2020, **18**, 577–594, DOI: **10.1007/s10311-020-00963-5**.

6 Y. Zhu, Y. Zhang and Y. Zhou, Application Progress of Modified Chitosan and Its Composite Biomaterials for Bone Tissue Engineering, *Int. J. Mol. Sci.*, 2022, **23**, 6574, DOI: **10.3390/ijms23126574**.

7 M. A. Mohammed, J. T. M. Syeda, K. M. Wasan and E. K. Wasan, An overview of chitosan nanoparticles and its application in non-parenteral drug delivery, *Pharmaceutics*, 2017, 53, DOI: **10.3390/pharmaceutics9040053**.

8 C. C. Thong, D. C. L. Teo and C. K. Ng, Application of polyvinyl alcohol (PVA) in cement-based composite materials: A review of its engineering properties and microstructure behavior, *Constr. Build. Mater.*, 2016, **107**, 172–180, DOI: **10.1016/J.CONBUILDMAT.2015.12.188**.

9 M. Ye, P. Mohanty and G. Ghosh, Morphology and properties of poly vinyl alcohol (PVA) scaffolds: Impact of process variables, *Mater. Sci. Eng., C*, 2014, **42**, 289–294, DOI: **10.1016/J.MSEC.2014.05.029**.

10 B. Kaur and D. Chakraborty, Biotechnological and molecular approaches for vanillin production: A review, *Appl. Biochem. Biotechnol.*, 2013, **169**, 1353–1372, DOI: **10.1007/S12010-012-0066-1**.

11 C. Huang, H. Liao, X. Liu, M. Xiao, S. Liao, S. Gong, F. Yang, X. Shu and X. Zhou, Preparation and characterization of vanillin-chitosan Schiff base zinc complex for a novel Zn2+ sustained released system, *Int. J. Biol. Macromol.*, 2022, **194**, 611–618, DOI: **10.1016/J.IJBIOMAC.2021.11.104**.

12 M. Mirhaj, M. Tavakoli, J. Varshosaz, S. Labbaf, S. Salehi, A. Talebi, N. Kazemi, V. Haghighi and M. Alizadeh, Preparation of a biomimetic bi-layer chitosan wound dressing composed of A-PRF/sponge layer and L-arginine/nanofiber, *Carbohydr. Polym.*, 2022, **292**, 119648, **https://www.sciencedirect.com/science/article/pii/S0144861722005537**.

13 P. Heydari, J. Varshosaz, M. Kharaziha and S. H. Javanmard, Antibacterial and pH-sensitive methacrylate poly-L-Arginine/poly (β-amino ester) polymer for soft tissue engineering, *J. Mater. Sci.: Mater. Med.*, 2023, **34**, 16, DOI: **10.1007/S10856-023-06720-8**.

14 H. S. Oh, S. K. Oh, J. S. Lee, C. Wu and S. J. Lee, Effects of l-arginine on growth hormone and insulin-like growth factor 1, *Food Sci. Biotechnol.*, 2017, **26**, 1749–1754, DOI: **10.1007/S10068-017-0236-6**.

15 H. Tapiero, G. Mathé, P. Couvreur, K. D. Tew and I. Arginine, *Biomed. Pharmacother.*, 2002, **56**, 439–445, DOI: **10.1016/S0753-3322(02)00284-6**.

16 C. Xu, W. Zhan, X. Tang, F. Mo, L. Fu and B. Lin, Self-healing chitosan/vanillin hydrogels based on Schiff-base bond/hydrogen bond hybrid linkages, *Polym. Test.*, 2018, **66**, 155–163, **https://www.sciencedirect.com/science/article/pii/S0142941817318512**.

17 I. Sani Mamman, Y. Y. Teo and M. Misran, Synthesis, characterization and rheological study of Arabic gum-grafted-poly (methacrylic acid) hydrogels, *Polym. Bull.*, 2021, **78**, 3399–3423, DOI: **10.1007/S00289-020-03267-4**.

18 S. A. Salim, N. M. Badawi, S. H. EL-Moslamy, E. A. Kamoun and B. A. Daihom, Novel long-acting brimonidine tartrate loaded-PCL/PVP nanofibers for versatile biomedical applications: fabrication, characterization and antimicrobial evaluation, *RSC Adv.*, 2023, **13**, 14943–14957, DOI: **10.1039/d3ra02244g**.

19 M. M. Abdul-Monem, E. A. Kamoun, D. M. Ahmed, E. M. El-Fakharany, F. H. Al-Abbassy and H. M. Aly, Light-cured hyaluronic acid composite hydrogels using riboflavin as a photoinitiator for bone regeneration applications, *J. Taibah Univ. Med. Sci.*, 2021, **16**, 529–539, DOI: **10.1016/J.JTUMED.2020.12.021**.

20 H. M. Abdel-Mageed, D. Nada, R. A. Radwan, S. A. Mohamed and N. A. E. L. Gohary, Optimization of catalytic properties of Mucor racemosus lipase through immobilization in a biocompatible alginate gelatin hydrogel matrix for free fatty acid production: a sustainable robust biocatalyst for ultrasound-assisted olive oil hydrolysis, *3 Biotech*, 2022, **12**, 1–16, DOI: **10.1007/S13205-022-03319-8/FIGURES/6**.

21 E. A. Kamoun, N-succinyl chitosan–dialdehyde starch hybrid hydrogels for biomedical applications, *J. Adv. Res.*, 2016, **7**, 69–77, DOI: **10.1016/J.JARE.2015.02.002**.

22 S. A. Salim, E. A. Kamoun, S. Evans, S. H. El-Moslamy, E. M. El-Fakharany, M. M. Elmazar, A. F. Abdel-Aziz, R. H. Abou-Saleh and T. A. Salaheldin, Mercaptopurine-loaded sandwiched tri-layered composed of electrospun polycaprolactone/poly (Methyl methacrylate) nanofibrous scaffolds as anticancer carrier with antimicrobial and antibiotic features: Sandwich configuration nanofibers, release study and *in vitro* bioevaluation tests, *Int. J. Nanomed.*, 2021, **16**, 6937–6955, DOI: **10.2147/IJN.S332920**.

23 N. A. Al-Dhabi, A. K. M. Ghilan, M. V. Arasu and V. Duraipandiyan, Green biosynthesis of silver nanoparticles produced from marine Streptomyces sp. Al-Dhabi-89 and their potential applications against wound infection and drug resistant clinical pathogens, *J. Photochem. Photobiol., B*, 2018, **189**, 176–184, DOI: **10.1016/J.JPHOTOBIOL.2018.09.012**.

24 A. Mounika, M. Sushma, L. Sidde, S. Malathi and K. Rajani, In vitro evaluation of antimicrobial activity of Clove buds

(Euginea aromatica), *Int. J. Indig. Herbs Drugs*, 2020, **5**, 25–33, DOI: 10.46956/ijihd.vi.95.

25 A. K. K. Noorafsha, A. Kashyap, L. Deshmukh and D. Vishwakarma, Biosynthesis and biophysical elucidation of CuO nanoparticle from Nyctanthes arbor-tristis Linn Leaf, *Appl. Microbiol. Biotechnol.*, 2022, **106**, 5823–5832, DOI: 10.1007/S00253-022-12105-8.

26 M. P. Weinstein, J. S. Lewis, A. M. Bobenchik, *et al.*, *Performance Standards for Antimicrobial Susceptibility Testing: M100*, Clinical and Laboratory Standars Institute, 30th edn, 2019, vol. 40(1).

27 A. Minich, Z. Levarski, M. Mikulášová, M. Straka, A. Liptáková and S. Stuchlík, Complex Analysis of Vanillin and Syringic Acid as Natural Antimicrobial Agents against Staphylococcus epidermidis Biofilms, *Int. J. Mol. Sci.*, 2022, **23**, 1816, DOI: 10.3390/IJMS23031816.

28 A. M. Shehabeldine, B. H. Amin, F. A. Hagras, A. A. Ramadan, M. R. Kamel, M. A. Ahmed, K. H. Atia and S. S. Salem, Potential Antimicrobial and Antibiofilm Properties of Copper Oxide Nanoparticles: Time-Kill Kinetic Essay and Ultrastructure of Pathogenic Bacterial Cells, *Appl. Biochem. Biotechnol.*, 2023, **195**, 467–485, DOI: 10.1007/S12010-022-04120-2.

29 Y. Y. Loo, Y. Rukayadi, M. A. R. Nor-Khaizura, C. H. Kuan, B. W. Chieng, M. Nishibuchi and S. Radu, *In Vitro* antimicrobial activity of green synthesized silver nanoparticles against selected Gram-negative foodborne pathogens, *Front. Microbiol.*, 2018, **9**, 1555, DOI: 10.3389/FMICB.2018.01555/FULL.

30 R. Yuniarti, S. Nadia, A. Alamanda, M. Zubir, R. A. Syahputra and M. Nizam, Characterization, Phytochemical Screenings and Antioxidant Activity Test of Kratom Leaf Ethanol Extract (Mitragyna speciosa Korth) Using DPPH Method, *J. Phys.: Conf. Ser.*, 2020, **1462**, 012026.

31 A. Hassani, S. Mahmood, H. H. Enezei, S. A. Hussain, H. A. Hamad, A. F. Aldoghachi, A. Hagar, A. A. Doolaanea and W. N. Ibrahim, Formulation, Characterization and Biological Activity Screening of Sodium Alginate-Gum Arabic Nanoparticles Loaded with Curcumin, *Molecules*, 2020, **25**, 2244, DOI: 10.3390/MOLECULES25092244.

32 T. Mosmann, Rapid colorimetric assay for cellular growth and survival: Application to proliferation and cytotoxicity assays, *J. Immunol. Methods*, 1983, **65**, 55–63, DOI: 10.1016/0022-1759(83)90303-4.

33 B. S. El-Menshawi, W. Fayad, K. Mahmoud, S. M. El-Hallouty, M. El-Manawaty, M. H. Olofsson and S. Linder, Screening of natural products for therapeutic activity against solid tumors, *Indian J. Exp. Biol.*, 2010, **48**(03), 258–264, http://nopr.niscpr.res.in/handle/123456789/7402, accessed March 10, 2024.

34 M. I. Thabrew, R. D. Hughes and I. G. Mcfarlane, Screening of Hepatoprotective Plant Components using a HepG2 Cell Cytotoxicity Assay, *J. Pharm. Pharmacol.*, 1997, **49**, 1132–1135, DOI: 10.1111/J.2042-7158.1997.TB06055.X.

35 Y. Hussein, E. M. El-Fakharany, E. A. Kamoun, S. A. Loutfy, R. Amin, T. H. Taha, S. A. Salim and M. Amer, Electrospun PVA/hyaluronic acid/L-arginine nanofibers for wound healing applications: Nanofibers optimization and *in vitro* bioevaluation, *Int. J. Biol. Macromol.*, 2020, **164**, 667–676, DOI: 10.1016/J.IJBIOMAC.2020.07.126.

36 R. Li, S. Ye, P. Ni, J. Shan, T. Yuan and J. Liang, Vanillin enhances the antibacterial and antioxidant properties of polyvinyl alcohol-chitosan hydrogel dressings, *Int. J. Biol. Macromol.*, 2022, **220**, 109–116.

37 Y. Cao, C. Qin, Z. Zhao and Z. Wang, Preparation and Properties of Medium-Density Fiberboards Bonded with Vanillin Crosslinked Chitosan, *Polymers*, 2023, **15**(11), 2509, https://www.mdpi.com/2073-4360/15/11/2509.

38 G. Michailidou, E. N. Koukaras and D. N. Bikiaris, Vanillin chitosan miscible hydrogel blends and their prospects for 3D printing biomedical applications, *Int. J. Biol. Macromol.*, 2021, **192**, 1266–1275, DOI: 10.1016/j.ijbiomac.2021.10.093.

39 R. L. C. G. da Silva, O. D. Bernardinelli, E. C. G. Frachini, H. Ulrich, E. Sabadini and D. F. S. Petri, Vanillin crosslinked chitosan films: The states of water and the effect of carriers on curcumin uptake, *Carbohydr. Polym.*, 2022, **292**, 119725, DOI: 10.1016/j.carbpol.2022.119725.

40 Y. Cao, C. Qin, Z. Zhao, Z. Wang and C. Jin, Preparation and Properties of Medium-Density Fiberboards Bonded with Vanillin Crosslinked Chitosan, *Polymers*, 2023, **15**, 2509, DOI: 10.3390/polym15112509.

41 G. H. Matar, E. Kaymazlar, M. Andac and O. Andac, Novel Binary Blended Hydrogel Films (Chitosan-Vanillin Schiff Base/Locust Bean Gum and Fe(III), Cu(II) & Zn(II) Complexes): Synthesis, Characterization, Conductivity, and Antibacterial Activity, *J. Polym. Environ.*, 2023, **31**, 3509–3521, DOI: 10.1007/S10924-023-02822-0/METRICS.

42 N. Akhlaghi and G. Najafpour-Darzi, Thermosensitive injectable dual drug-loaded chitosan-based hybrid hydrogel for treatment of orthopedic implant infections, *Carbohydr. Polym.*, 2023, **320**, 121138, DOI: 10.1016/J.CARBPOL.2023.121138.

43 M. Eldin and E. Kamoun, L-Arginine grafted alginate hydrogel beads: A novel pH-sensitive system for specific protein delivery, *Arabian J. Chem.*, 2015, **8**(3), 355–365, https://www.sciencedirect.com/science/article/pii/S1878535214000100.

44 H. Ashraf, S. A. Salim, S. H. EL-Moslamy, S. A. Loutfy and E. A. Kamoun, An Injectable *In Situ* Forming Collagen/Alginate/CaSO4 Composite Hydrogel for Tissue Engineering Applications: Optimization, Characterization and *In Vitro* Assessments, *Arabian J. Sci. Eng.*, 2024, 1–15, DOI: 10.1007/s13369-024-08922-w.

45 Y. Hussein, E. A. Kamoun, S. A. Loutfy, R. Amin, E. M. El-Fakharany, T. H. Taha and M. Amer, Physically and chemically-crosslinked L-arginine-loaded polyvinyl alcohol-hyaluronic acid- cellulose nanocrystals hydrogel membranes for wound healing: influence of crosslinking methods on biological performance of membranes *in Vitro*, *J. Umm Al-Qura Univ. Appl. Sci.*, 2023, **9**, 304–316, DOI: 10.1007/S43994-023-00045-6.

46 H. Kaya, O. Bulut, A. R. Kamali and D. Ege, l-Arginine modified multi-walled carbon nanotube/sulfonated poly(ether ether ketone) nanocomposite films for

biomedical applications, *Appl. Surf. Sci.*, 2018, **444**, 168–176, DOI: **10.1016/J.APSUSC.2018.03.046**.

47 M. Evcil and M. Karakaplan, Preparation, Characterization and Drug Release of Chitosan Hydrogels Derived From Substituted Salicylaldehyde, *ChemistrySelect*, 2023, **8**, e202204426, DOI: **10.1002/SLCT.202204426**.

48 C. Zou, T. Lu, R. Wang, P. Xu, Y. Jing, R. Wang, J. Xu and J. Wan, Comparative physiological and metabolomic analyses reveal that Fe3O4 and ZnO nanoparticles alleviate Cd toxicity in tobacco, *J. Nanobiotechnol.*, 2022, **20**, 302, DOI: **10.1186/S12951-022-01509-3**.

49 M. Sepahi, R. Jalal and M. M. Iranian, Antibacterial activity of poly-l-arginine under different conditions, *Iran. J. Microbiol.*, 2017, **9**(2), 103–111, **https://www.ncbi.nlm.nih.gov/pmc/articles/PMC5715275/**.

50 S. Rakchoy, P. Suppakul and T. Jinkarn, Antimicrobial effects of vanillin coated solution for coating paperboard intended for packaging bakery products, *Asian J. Food Agro Ind.*, 2009, **2**(04), 138–147, **https://www.cabdirect.org/cabdirect/abstract/20103303531**.

51 M. Arakha, S. Pal, D. Samantarrai, T. K. Panigrahi, B. C. Mallick, K. Pramanik, B. Mallick and S. Jha, Antimicrobial activity of iron oxide nanoparticle upon modulation of nanoparticle-bacteria interface, *Sci. Rep.*, 2015, **5**, 14813, DOI: **10.1038/SREP14813**.

52 E. Cruz, da S. Ferreira, L. Fabrício Bahia Nogueira, M. Antônio Eufrásio Cruz, G. José Aguilar, D. Rita Tapia-Blácido, M. Eliana da Silva Ferreira, B. Chieregato Maniglia, M. Bottini, P. Ciancaglini and A. Paula Ramos, Synthesis of Antibacterial Hybrid Hydroxyapatite/Collagen/Polysaccharide Bioactive Membranes and Their Effect on Osteoblast Culture, *Int. J. Mol. Sci.*, 2022, 7277, DOI: **10.3390/ijms23137277**.

53 A. Ismail Saheb, N. Habibi, A. A. Ismail, L. Al-Hajji, I. Azad, A. Al-Yaqoot, N. Habibi, M. Alseidi and S. Ahmed, Self-cleaning application of mesoporous ZnO, TiO_2 and Fe_2O_3 films with the accommodation of silver nanoparticles for antibacterial activity, *J. Taiwan Inst. Chem. Eng.*, 2023, **142**, 104627, DOI: **10.1016/j.jtice.2022.104627**.

54 M.-M. Iftime, I. Rosca, A.-I. Sandu and L. Marin, Chitosan crosslinking with a vanillin isomer toward self-healing hydrogels with antifungal activity, *Int. J. Biol. Macromol.*, 2022, **205**, 574–586, DOI: **10.1016/j.ijbiomac.2022.02.077**.

55 A. Minich, Z. Levarski, M. Mikulášová, M. Straka, A. Liptáková and S. Stuchlík, Complex Analysis of Vanillin and Syringic Acid as Natural Antimicrobial Agents against Staphylococcus epidermidis Biofilms, *Int. J. Mol. Sci.*, 2022, **23**, 1816, DOI: **10.3390/ijms23031816**.

56 S. Rakchoy, P. Suppakul and T. Jinkarn, Antimicrobial effects of vanillin coated solution for coating paperboard intended for packaging bakery product, *Asian J. Food Agro Ind.*, 2009, **2**, 138–147.

57 C. Zou, T. Lu, R. Wang, P. Xu, Y. Jing, R. Wang, J. Xu and J. Wan, Comparative physiological and metabolomic analyses reveal that Fe3O4 and ZnO nanoparticles alleviate Cd toxicity in tobacco, *J. Nanobiotechnol.*, 2022, **20**, 1–22, DOI: **10.1186/s12951-022-01509-3**.

58 M. Sepahi, R. Jalal and M. Mashreghi, Antibacterial activity of poly-l-arginine under different conditions, *Iran. J. Microbiol.*, 2017, **9**, 103–111.